NASA TECHNICAL MEMORANDUM

NASA TM X-3108

NASA TM X-3108

CONTROL SYSTEM DESIGN USING FREQUENCY DOMAIN MODELS AND PARAMETER OPTIMIZATION, WITH APPLICATION TO SUPERSONIC INLET CONTROLS

by Robert C. Seidel and Bruce Lehtinen

Lewis Research Center
Cleveland, Ohio 44135

NATIONAL AERONAUTICS AND SPACE ADMINISTRATION • WASHINGTON, D. C. • OCTOBER 1974

1. Report No.	2. Government Accession No.	3. Recipient's Catalog No.
NASA TM X-3108		

4. Title and Subtitle	5. Report Date
CONTROL SYSTEM DESIGN USING FREQUENCY DOMAIN MODELS AND PARAMETER OPTIMIZATION, WITH APPLICATION TO SUPERSONIC INLET CONTROLS	OCTOBER 1976
	6. Performing Organization Code
7. Author(s)	8. Performing Organization Report No.
Robert C. Seidel and Bruce Lehtinen	E-7710
	10. Work Unit No.
9. Performing Organization Name and Address	501-24
Lewis Research Center	11. Contract or Grant No.
National Aeronautics and Space Administration	
Cleveland, Ohio 44135	13. Type of Report and Period Covered
12. Sponsoring Agency Name and Address	Technical Memorandum
National Aeronautics and Space Administration	14. Sponsoring Agency Code
Washington, D. C. 20546	

15. Supplementary Notes

16. Abstract

A technique is described for designing feedback control systems using frequency domain models, a quadratic cost function, and a parameter optimization computer program. FORTRAN listings for the computer program are included in the report. The approach is applied to the design of shock position controllers for a supersonic inlet. Considered are a deterministic or random system disturbance and the presence of random measurement noise. The cost function minimized is formulated in the time domain, but the problem solution is obtained using a frequency domain system description. A scaled and constrained conjugate gradient algorithm is used for the minimization. In applying the approach to a typical supersonic inlet, both optimal proportional-plus-integral (PI) and proportional-plus-integral-plus-derivative (PID) controllers were calculated. For the inlet considered, a single-loop PI controller was judged to be the most desirable of the various designs considered.

17. Key Words (Suggested by Author(s))		18. Distribution Statement
Control	Frequency domain	Unclassified - unlimited
Parameter optimization	Gradient search	Category 08
Supersonic inlet		

19. Security Classif. (of this report)	20. Security Classif. (of this page)	21. No. of Pages	22. Price*
Unclassified	Unclassified	50	$3.25

CONTROL SYSTEM DESIGN USING FREQUENCY DOMAIN MODELS AND PARAMETER OPTIMIZATION, WITH APPLICATION TO SUPERSONIC INLET CONTROLS

by Robert C. Seidel and Bruce Lehtinen

Lewis Research Center

SUMMARY

This report described a technique for designing feedback control systems using frequency domain models, a quadratic performance index, and a parameter optimization computer program. The approach is applied to the design of a terminal shock position controller for a mixed-compression supersonic inlet. The computer program described can be used to design controllers for any two-loop linear feedback system having a single control input and a cascade structure. The problem formulation assumes the system is acted upon by a single deterministic or random disturbance plus random measurement noise introduced in each loop. The quadratic performance index chosen to be minimized is a weighted sum of averaged square system output, output rate, control, and control rate. The performance index is expressed in the frequency domain and is minimized, given a frequency domain system description, using a scaled and constrained conjugate gradient search algorithm.

For the supersonic inlet problem, the disturbance is a deterministic airflow perturbation at the diffuser exit, and measurement noises are assumed to contaminate inlet duct pressure measurements. The cost function chosen to be minimized is a weighted sum of averaged square values of the output (throat exit static pressure) and its derivative plus the control (inlet bypass door area) and its derivative. Optimal parameters were calculated for both proportional-plus-integral (PI) and proportional-plus-integral-plus-derivative (PID) single-loop controllers for a NASA designed mixed compression inlet. Feedback signals used were either throat exit static or diffuser exit static pressures. Designs were evaluated on the basis of averaged square values of output and control signals. PI control on throat exit static pressure proved to be the most effective compromise between complexity and ability to attenuate disturbances. Appendixes are included to describe the computer program as well as outline the solution to a sample design problem.

A supersonic aircraft propulsion system consists of a supersonic inlet and either a turbofan or turbojet engine. The function of the inlet is to convert high velocity, low pressure air ahead of the inlet to low velocity, high pressure air more suitable for the engine's compressor. An efficient inlet for flight at Mach numbers above about 2 is the mixed compression type, having a convergent supersonic region followed by a divergent subsonic region. An increase in static pressure occurs in both regions as the flow is decelerated. A terminal shock separates the supersonic and subsonic flows. To maximize efficiency, the terminal shock should be located near the throat in the divergent duct. If the terminal shock moves upstream into the convergent region, it jumps forward to form a strong shock wave ahead of the inlet. This occurrence is known as an inlet unstart, and results in increased drag and a rapid loss in pressure recovery. This in turn may lead to a compressor stall and/or combustor flameout. Conversely, if the shock moves too far downstream, the pressure recovery is reduced and distortion is increased at the compressor face, which may also cause compressor stall. Thus, controls are needed to maintain the terminal shock close to but yet downstream of the throat for good pressure recovery without inlet unstarts.

Figure 1 is a schematic diagram of a mixed compression inlet with a typical terminal shock control loop shown. The terminal shock is positioned using the bypass door loop. The door opens and closes to maintain a match between the inlet and engine airflow as engine airflow demand changes. This tends to prevent the terminal shock from moving too far rearward, causing increased distortion, or too far forward, causing an unstart. Throat exit and diffuser exit static pressure signals shown give indications of shock position. They are fed back through the controller to drive the bypass door servo.

The controller transfer functions are significant factors in the dynamic regulation of shock position. The design of such transfer functions has been studied in references 1 to 4. A root locus design technique was reported in reference 1. A stochastic optimal control theory approach was reported in references 2 and 3, where the expected frequency of unstarts was minimized. A parameter optimization approach, where the parameters in a fixed-form controller were selected so that the response approximated a desired closed-loop transfer function, was reported in reference 4.

The approach taken in this report is also based on optimizing the parameters in a fixed-form controller. However, the cost function chosen to be minimized is the weighted sum of average integral square errors, due to a deterministic disturbance, and the mean square errors due to random noise on the measurements. This approach was motivated by the inlet control problem (ref. 5), where the compressor face disturbance is most conveniently described as a deterministic signal but where the noise on duct pressure measurements is definitely random in nature. The variables included in the

spective first derivatives.

While the problem is formulated in the time domain, the optimization is done in the frequency domain. This is because system, disturbance, and noise models are most often obtained in frequency domain form. The conjugate gradient search (ref. 6) is used for the optimization. However, the standard procedure is modified to reduce search convergence time and insure that the resulting controller is stable. This is done by scaling and constraining the search parameters.

In the next section, the general control problem investigated is defined and the cost function and gradient calculations are described. Then the parameter optimization program used is described, followed by a description of the inlet model to which the controller design method was applied. Finally, the results are presented, followed by appendixes, which include one on the use of the computer program and one in which a sample problem is presented.

GENERAL CONTROL PROBLEM DESCRIPTION

Description of Plant, Noise, and Disturbance

Motivated by the supersonic inlet control problem, a control system structure was selected as a framework for the controller design problem. This structure is shown in figure 2. The linear plant (blocks G_1 and G_2) is assumed to have two measurements x_1 and x_2 available. (Symbols are defined in appendix A.) Variable x_1, the outer-loop measurement, is considered the output. The control is to consist of two blocks, H_1 and H_2, whose forms are specified at the outset, but whose parameters are to be optimized. The two inputs to the controller are assumed contaminated with independent Gaussian noises v_1 and v_2, each having the same power spectral density $\Phi_v(\omega)$. The controller output drives actuator G_a to produce control u. The plant is acted upon by deterministic disturbance d which occurs at time zero.

Cost Function Evaluation

It is assumed that the purpose of the controller is to keep x_1 and $\dot{x}_1$ as close to zero as possible but at the same time limiting the excursions in control u and control rate $\dot{u}$. Thus, a cost function must be defined which adequately reflects the average deviations in output and control caused by random measurement noises v_1 and v_2 and deterministic disturbance d. We now proceed to develop such a cost function.

For convenience, define components of x_1 and u such that

$$\left.\begin{aligned} x_1 &= x_{1v} + x_{1d} \\ \dot{x}_1 &= \dot{x}_{1v} + \dot{x}_{1d} \\ u &= u_v + u_d \\ \dot{u} &= \dot{u}_v + \dot{u}_d \end{aligned}\right\} \tag{1}$$

where the first quantities on the right sides of equation (1) are the components due to measurement noise v_1 and v_2 and the second quantities on the right sides are components due to deterministic disturbance d. First, separate cost functions will be derived for the measurement noise and deterministic inputs. Then, these separate cost functions will be combined into a single cost function. Consider first the case where only measurement noise is present. Define the cost function

$$C_v = \lim_{\tau \to \infty} \frac{1}{2\tau} \int_{-\tau}^{\tau} \left[q_1 x_{1v}^2(t) + q_2 \dot{x}_{1v}^2(t) + r_1 u_v^2(t) + r_2 \dot{u}_v^2(t) \right] dt \tag{2}$$

The q's and r's are arbitrarily selected scalar penalties. Thus, C_v is simply a weighted sum of mean square values. Next, consider the case where only a deterministic disturbance d is present. Disturbance d is assumed to be zero for $t < 0$. Define the cost function

$$C_d = \frac{1}{T} \int_0^T \left[q_1 x_{1d}^2(t) + q_2 \dot{x}_{1d}^2(t) + r_1 u_d^2(t) + r_2 \dot{u}_d^2(t) \right] dt \tag{3}$$

Time T is defined as the (arbitrarily selected) period during which control is to be effective in minimizing the effects of d. Factor $1/T$ is included to make C_d an <u>average</u> integral squared quantity, and thus comparable to mean square quantity C_v. Now, the total cost function can be defined as

$$C = C_v + C_d \tag{4}$$

Cost function C is to be minimized by proper selection of controller transfer function parameters. The problem may be simplified if we assume that T is large enough so

that x_{1d}, $\dot{x}_{1d}$, u_d, and $\dot{u}_d$ all go to zero before $t = T$. Then the total cost can be written as

$$C = C_v + C_{d\infty} \tag{5}$$

$$C = \lim_{\tau \to \infty} \frac{1}{2\tau} \int_{-\tau}^{\tau} \left[q_1 x_{1v}^2(t) + q_2 \dot{x}_{1v}^2(t) + r_1 u_v^2(t) + r_2 \dot{u}^2(t) \right] dt$$

$$+ \frac{1}{T} \int_0^{\infty} \left[q_1 x_{1d}^2(t) + q_2 \dot{x}_{1d}^2(t) + r_1 u_d^2(t) + r_2 \dot{u}_d^2(t) \right] dt \tag{6}$$

where the upper limit on the second integral $C_{d\infty}$ has now been made equal to ∞.

Our aim is now to express C in the frequency domain, since, as was indicated previously, we desire to perform the parameter optimization using frequency domain system models and data. In the following development, an expression for C will be obtained which is an integral in the frequency domain, over a range of 0 to ∞. The integrand will be obtained in terms of the following known quantities: noise power spectral density (PSD), plant, and controller transfer functions, and the Fourier transform of the disturbance.

As previously noted, cost function C_v (eq. (2)) is a weighted sum of mean square values of stationary random variables x_{1v}, $\dot{x}_{1v}$, u_v, and $\dot{u}_v$. It can be shown (ref. 7) that the mean square value of any stationary random variable y can be expressed in the frequency domain as

$$\overline{y^2} = \lim_{\tau \to \infty} \frac{1}{2\tau} \int_{-\tau}^{\tau} y^2(t) dt = \frac{1}{2\pi} \int_{-\infty}^{\infty} \Phi_y(\omega) d\omega \tag{7}$$

where $\overline{y^2}$ is defined as the mean square value of y and $\Phi_y(\omega)$ is defined as the PSD of y. It can also be shown (ref. 7) that the PSD of the output of a single-input - single-output linear system whose transfer function is $G(s)$ is given by

$$\Phi_y(\omega) = \Phi_z(\omega) \left| G(j\omega) \right|^2 \tag{8}$$

where $\Phi_z(\omega)$ is the PSD of the input to the system. If the system of concern is a differentiator, that is, $G(s) = s$, or $y(s) = s\, z(s)$, then $\Phi_y(\omega) = \omega^2 \Phi_z(\omega)$. We can use this fact plus equation (7) to express C_v in terms of PSD's, obtaining

$$C_v = \frac{1}{2\pi}\int_{-\infty}^{\infty}\left[\left(q_1 + \omega^2 q_2\right)\Phi_{x_1}(\omega) + \left(r_1 + \omega^2 r_2\right)\Phi_u(\omega)\right]d\omega \tag{9}$$

where $\Phi_{x_1}(\omega)$ is the PSD of x_{1v} and $\Phi_u(\omega)$ is the PSD of u_v.

Next we must express $C_{d\infty}$ in terms of frequency dependent variables. Given a time function $y(\tau)$, having a Fourier transform $y(j\omega)$, Parseval's theorem (ref. 7) states that

$$\int_{-\infty}^{\infty} y(t)^2\,dt = \frac{1}{2\pi}\int_{-\infty}^{\infty}|y(j\omega)|^2\,d\omega \tag{10}$$

Then $C_{d\infty}$ of equation (6) can be put in the form of the left side of equation (10) by allowing the lower limit in equation (6) be $-\infty$. This can be done because the integrand of $C_{d\infty}$ is zero for time $t < 0$. If this fact is used in addition to $\dot{y}(j\omega) = j\omega\, y(j\omega)$, a frequency domain expression can be obtained for $C_{d\infty}$ as

$$C_{d\infty} = \frac{1}{2\pi T}\int_{-\infty}^{\infty}\left[\left(q_1 + \omega^2 q_2\right)|x_{1d}(j\omega)|^2 + \left(r_1 + \omega^2 r_2\right)|u_d(j\omega)|^2\right]d\omega \tag{11}$$

Since the integrands of equations (9) and (11) are even functions of frequency, the lower limits can be set to zero, and an expression for cost function C obtained as

$$C = \frac{1}{\pi}\int_0^{\infty}\left\{\left[\left(q_1 + \omega^2 q_2\right)\Phi_{x_1}(\omega) + \left(r_1 + \omega^2 r_2\right)\Phi_u(\omega)\right]\right\}$$

$$+ \frac{1}{T}\left\{\left[\left(q_1 + \omega^2 q_2\right)|x_{1d}(j\omega)|^2 + \left(r_1 + \omega^2 r_2\right)|u_d(j\omega)|^2\right]\right\}d\omega \tag{12}$$

To be able to numerically evaluate C, the PSD's and the absolute value squares must be expressed in terms of known system transfer functions, noise PSD $\Phi_v(\omega)$, and disturbance Fourier transform absolute value squared, $|d(j\omega)|^2$. Refer now to figure 2. First, variable x_{1v}, the component of u_1 due to measurement noise, can be written as

$$x_{1v}(s) = G_a(s)G_{cl}(s)\left[H_1(s)v_1(s) + H_2(s)v_2(s)\right] \tag{13}$$

where

$$G_{cl}(s) = \frac{G_1(s)G_2(s)}{1 + G_s(s)\left[G_1(s)H_2(s) + G_1(s)G_2(s)H_1(s)\right]} \tag{14}$$

Variable x_{1d}, the component of x_1 due to the disturbance, is

$$x_{1d}(s) = G_{cl}(s)\, d(s) \tag{15}$$

Similarly, the component of u due to measurement noise is

$$u_v(s) = \frac{G_{cl}(s)G_a(s)}{G_1(s)G_2(s)}\left[H_1(s)v_1(s) + H_2(s)v_2(s)\right] \tag{16}$$

and the component of u due to the disturbance is

$$u_d(s) = G_{cl}(s)G_a(s)\left[\frac{H_2(s)}{G_2(s)} + H_1(s)\right]d(s) \tag{17}$$

Using equations (13) and (16), the fact that v_1 and v_2 are uncorrelated, and letting $s = j\omega$, the PDS's of x_{1v} and u_v become

$$\Phi_{x_{1v}}(\omega) = \Phi_v(\omega)\left|G_a(j\omega)G_{cl}(j\omega)\right|^2\left[\left|H_1(j\omega)\right|^2 + \left|H_2(j\omega)\right|^2\right] \tag{18}$$

and

$$\Phi_{u_v}(\omega) = \Phi_v(\omega)\left|\frac{G_{cl}(j\omega)G_a(j\omega)}{G_1(j\omega)G_2(j\omega)}\right|^2\left[\left|H_1(j\omega)\right|^2 + \left|H_2(j\omega)\right|^2\right] \tag{19}$$

Also, using equation (15) results in

$$\left|x_{1d}(j\omega)\right|^2 = \left|G_{cl}(j\omega)\right|^2\left|d(j\omega)\right|^2 \tag{20}$$

and using equation (17) gives

$$u_d(j\omega)^2 = |G_{cl}(j\omega)G_a(j\omega)|^2 \left|\frac{H_2(j\omega)}{G_2(j\omega)} + H_1(j\omega)\right|^2 |d(j\omega)|^2 \tag{21}$$

Substituting equations (18) to (21) into the cost function equation (12), cost C becomes

$$C = C(\underline{b}) = \frac{1}{\pi}\int_0^\infty F(\omega,\underline{b})d\omega \tag{22}$$

where $F(\omega,\underline{b})$ is defined as

$$F(\omega,\underline{b}) \triangleq |G_{cl}(j\omega,\underline{b})|^2 \left\{\left[V_q(\omega) + V_r(\omega)\right]\left[|H_1(j\omega,\underline{b})|^2 + |H_2(j\omega,\underline{b})|^2\right] + D_q(\omega) + D_r(\omega)\left|\frac{H_2(j\omega,\underline{b})}{G_2(j\omega)} + H_1(j\omega,\underline{b})\right|^2\right\} \tag{23}$$

and

$$\left.\begin{aligned} V_q(\omega) &\triangleq \left(q_1 + \omega^2 q_2\right)\Phi_v(\omega)|G_a(j\omega)|^2 \\ V_r(\omega) &\triangleq \left(r_1 + \omega^2 r_2\right)\Phi_v(\omega)\left|\frac{G_a(j\omega)}{G_1(j\omega)G_2(j\omega)}\right|^2 \\ D_q(\omega) &\triangleq \frac{1}{T}\left(q_1 + \omega^2 q_2\right)|d(j\omega)|^2 \\ D_r(\omega) &\triangleq \frac{1}{T}\left(r_1 + \omega^2 r_2\right)|d(j\omega)|^2|G_a(j\omega)|^2 \end{aligned}\right\} \tag{24}$$

The symbolism $H_1(j\omega,\underline{b})$ and so forth has been introduced to indicate which terms are functions of controller parameter vector $\underline{b}$. Note that $V_q(\omega)$, $V_r(\omega)$, $D_q(\omega)$, and $D_r(\omega)$ are all independent of the controller parameters.

Having now obtained an equation from which to evaluate C as a function of known system parameters and variable controller parameters, the parameter optimization problem to be solved is: minimize $C(\underline{b})$ by proper selection of parameter vector $\underline{b}$.

The problem has thus far been formulated for the case where the system is acted upon by a single deterministic disturbance plus two random measurement noises. However, the problem can be considered to be a completely stochastic one if the deterministic disturbance d(t) is replaced by a Gaussian random variable with a PSD of $\Phi_d(\omega)$. Then, $\Phi_d(\omega)$ would be used in place of $(1/T)|d(j\omega)|^2$ in equations (24). Also, the problem becomes entirely deterministic if measurement noise v is considered to be zero. In that case the noise PSD, $\Phi_v(\omega)$ is set to zero in equations (24).

Cost Function Gradient Evaluation

An expression for the cost function (eq. (22)) is not usually sufficient to allow an effective solution to the parameter optimization problem. Most parameter optimization methods (conjugate gradients, Fletcher-Powell, steepest descents, etc.) require also that the gradient of C be calculated. One way of computing an approximate gradient is to make finite perturbations in $\underline{b}$, compute C each time, and find the gradient as the change in C divided by the change in the respective $\underline{b}$ vector components. However, a more efficient method is to derive an explicit expression for the gradient ∇C in terms of $\underline{b}$. Such an approach was taken in this report. Equation (22) can be used to write the gradient as

$$\nabla C(\underline{b}) = \frac{1}{\pi} \int_0^\infty \nabla F(\omega, \underline{b}) d\omega \tag{25}$$

Using equations (23) and (14) makes it possible to express $\nabla F(\omega, \underline{b})$ as

$$\nabla F(\omega, \underline{b}) = 2\,\text{Real}\left[F(\omega, \underline{b}) \left\{ -G_{c\ell}(j\omega, \underline{b}) G_a(j\omega) \cdot \nabla \left[\frac{H_2(j\omega, \underline{b})}{G_2(j\omega)} + H_1(j\omega, \underline{b}) \right] \right\}^* \right.$$

$$+ |G_{c\ell}(j\omega, \underline{b})|^2 \left(D_r(\omega) \left[\frac{H_2(j\omega, \underline{b})}{G_2(j\omega)} + H_1(j\omega, \underline{b}) \right] \nabla \left[\frac{H_2(j\omega, \underline{b})}{G_2(j\omega)} + H_1(j\omega, \underline{b}) \right]^* \right.$$

$$\left. \left. + \left[V_q(\omega) + V_r(\omega) \right] \cdot \left\{ H_2(j\omega, \underline{b}) \nabla \left[H_2(j\omega, \underline{b}) \right]^* + H_1(j\omega, b) \nabla \left[H_1(j\omega, \underline{b}) \right]^* \right\} \right) \right] \tag{26}$$

where the fact that $\nabla|y(j\omega)|^2 = 2\,\text{Real}\,[y(j\omega)\nabla y(-j\omega)]$ was used. Once the forms of $H_1(j\omega,\underline{b})$ and $H_2(j\omega,\underline{b})$ have been chosen, the required gradients can also be calculated. In the computer program described in appendix B, $H_1(s,\underline{b})$ and $H_2(s,\underline{b})$ are assumed to be of the following form:

$$H_i(s,\underline{b}) = Kb_1 s^{m_1} \prod_{j=1}^{m_2}\left(\frac{s}{b_{2j}}+1\right)^{p_{2j}} \prod_{j=1}^{m_3}\left(\frac{s^2}{b_{4j}^2}+\frac{2sb_{3j}}{b_{4j}}+1\right)^{p_{3j}}, \qquad i = 1, 2 \tag{27}$$

Here, m_1, m_2, and m_3 are given. Exponents p_{2j} and p_{3j} indicate whether the factors appear in the numerator or denominator, are ± 1, and are given for all j. The parameter K could represent a transducer gain (for instance, conversion from a pressure measurement to a controller input voltage) and is given. With these restrictions, a closed form calculation can be made for $\nabla H_1(j\omega,\underline{b})$. For example, if $H_1(s,\underline{b})$ has four parameters and is given as

$$H_1(s,\underline{b}) = \frac{Kb_1}{s}\left(\frac{s}{b_{21}}+1\right)^{p_{21}}\left(\frac{s^2}{b_{41}^2}+\frac{2sb_{31}}{b_{41}}+1\right)^{p_{31}} \tag{28}$$

where $\underline{b}^T = (b_1, b_{21}, b_{31}, b_{41})$, then,

$$\nabla H_1(s,\underline{b}) = H_1(s,\underline{b}) \cdot \begin{bmatrix} \dfrac{1}{b_1} \\ \dfrac{-p_{21}s}{(s+b_{21})b_{21}} \\ \dfrac{2p_{31}s}{\left(\dfrac{s^2}{b_{41}^2}+\dfrac{2sb_{31}}{b_{41}}+1\right)b_{41}} \\ \dfrac{-2p_{31}\left(\dfrac{b_{31}}{b_{41}}+\dfrac{s^2}{b_{41}^2}\right)s}{\left(\dfrac{s^2}{b_{41}^2}+\dfrac{2sb_{31}}{b_{41}}+1\right)b_{41}} \end{bmatrix} \tag{29}$$

Programming Considerations

A computer program was written (see appendix B) which calculates the optimum parameters $\underline{b}$ using the conjugate gradient method (ref. 6). In the program, the cost function (eq. (22)) and cost function gradient (eq. (25)) are computed using numerical integration. In particular, using the trapezoidal rule, the cost function can be written as

$$C = \frac{1}{2\pi} \sum_{i=1}^{N_d} F(\omega_i)(\omega_{i+1} - \omega_{i-1}) \tag{30}$$

where N_d is the number of frequency points over which the integral is to be computed (≥ 3), ω_i is the frequency at the i^{th} data point, $\omega_{N_d+1} = \omega_{N_d}$, and $\omega_0 = \omega_1$. A similar expression can be written for the gradient. Judgment is required in selecting the spacing of the frequency points, such that integration errors are minimized. In addition, a variable step size feature is introduced to further reduce errors. This is done by using the fact that errors caused by a fixed step size are greatest near a system resonance. Resonance is defined herein as the portion where the closed-loop transfer function magnitude $|G_{c\ell}(s)|$ exceeds the open-loop transfer function magnitude. The program detects this condition and when it occurs, $|G_{c\ell}(j\omega)|^2$ is evaluated at additional points within each frequency interval using interpolation between adjacent prespecified frequency points. This feature increases accuracy and also tends to prevent occurrence of another computational problem, namely, that of the closed-loop system transfer function becoming unstable during the search. Since the magnitude squared of an unstable $G_{c\ell}(j\omega)$ is the same as a stable one having the same pole magnitudes, the cost function calculation won't differentiate between the desired stable and an unwanted unstable solution. However in becoming unstable during the search procedure, $G_{c\ell}(j\omega)$ will have an increasingly large resonant peak, which the program will tend to detect. Then the addition of the extra function values will ensure adequate accuracy in computing C and ∇C. That is, the decrease in system stability will be property reflected as an increase in the cost function.

The search procedure used is similar to the conjugate gradient method of reference 6. Two modifications were made to the conjugate gradient search to improve the speed of convergence in this application. The first was to constrain the search vector $\underline{b}$ components to not change sign. With the transfer functions defined by equation (27), this just means that only stable controllers are allowed as candidates for the optimal one. The second modification concerns scaling of the $\underline{b}$ vector. It is known that "spherical" cost functions (where the cost is more or less equally sensitive to each element of the $\underline{b}$ vector) tend to lend themselves to rapidly converging searches. Thus, a scaling was

incorporated into the search procedure such that each parameter has approximately equal influence. This was done by defining a new scaled parameter vector $\underline{p}$ using the diagonal matrix Λ as follows:

$$\underline{p} \triangleq \begin{bmatrix} 1/\lambda_1 & & & \\ & 1/\lambda_2 & & \\ & & \ddots & \\ & & & 1/\lambda_{m_p} \end{bmatrix} \cdot \underline{b} \triangleq \Lambda^{-1}\underline{b} \tag{31}$$

where λ_i is the magnitude of the i^{th} element of $\underline{b}$ at the end of the previous interation of the conjugate gradient algorithm. The cost function and gradient in terms of $\underline{p}$ are thus:

$$C(\underline{b}) = C(\Lambda\underline{p}) \tag{32}$$

and

$$\nabla F(\underline{p}) = \Lambda\ \nabla F(\underline{b}) \tag{33}$$

Theory states that the unmodified conjugate gradient search will always converge for quadratic cost functions. In the modified conjugate gradient search, the coordinate system is changed at the start of each iteration. Thus in theory, the modified conjugate gradient algorithm may not always converge for quadratic cost functions. However, experience to date on nonquadratic cost functions confirms that the aforementioned scaling algorithm gave convergence times less than or equal to those for nonscaled cases. Appendix C shows the results for one test case where scaling was particularly useful.

APPLICATION OF PARAMETER OPTIMIZATION TO INLET CONTROL DESIGN

The plant, to which the parameter optimization method is applied in this study, is a NASA designed two-dimensional, mixed-compression inlet. A description of the inlet is given in references 8 and 5. Reference 8 gives experimental open-loop frequency responses of the inlet's terminal shock and subsonic duct static pressures to overboard bypass door area. Experimental frequency responses of the inlet with control are given in

reference 5. In these tests, one set of overboard bypass doors was used to generate the disturbance and a second set was used for control.

Inlet and Noise Dynamics

The structure studied in this report is shown in figure 3. The output x_1 to be controlled is P_{57}, a throat exit static pressure 57 centimeters from the cowl lip and downstream of the terminal shock, which is used as an indication of shock position. Measured signal x_2 is pressure P_{87}, which is closer to the compressor face station, where the airflow rate disturbance d originates. Controllers H_1 and H_2 drive bypass doors G_a which pass more or less flow to counteract the effects of disturbance d. Control u is u_{bp}, bypass door area (or airflow rate).

The inlet dynamics and bypass door frequency responses were found in reference 8 and are tabulated in table I. Magnitude data are shown normalized to the values at 1 hertz. Experimental frequency response data were available over the range of 1 to 150 hertz; points at 0.001, 300, and 600 hertz were extrapolated using transfer function models similar to those given in reference 8.

From a limited amount of experimental data, measurement noises v_1 and v_2 were found to be uncorrelated and to have the same PSD $\Phi_v(\omega)$. The PSD is tabulated in table I, with the data for 300 and 600 hertz extrapolated to be equal to the value at 150 hertz.

Cost Function

To simplify the discussion of results, the cost function of equation (12), by substituting and collecting terms, can be written in terms of averaged square values as

$$C = q_1\overline{x_1^2} + q_2\overline{\dot{x}_1^2} + r_1\overline{u^2} + u_2\overline{\dot{u}_2^2} \tag{34}$$

where

$$\overline{x_1^2} \triangleq \frac{1}{\pi}\int_0^\infty \left[\Phi_{x_{1v}}(\omega) + \frac{1}{T}\left|x_{1d}(j\omega)\right|^2\right]d\omega \triangleq \text{averaged square output} \tag{35}$$

$$\overline{\dot{x}_1^2} \triangleq \frac{1}{\pi}\int_0^\infty \omega^2\left[\Phi_{x_{1v}}(\omega) + \frac{1}{T}\left|x_{1d}(j\omega)\right|^2\right]d\omega \triangleq \text{averaged square output rate} \tag{36}$$

$$\overline{u^2} \triangleq \frac{1}{\pi}\int_0^\infty \left[\Phi_u(\omega) + \frac{1}{T}\,|u_d(j\omega)|^2\right] d\omega \triangleq \text{averaged square control} \qquad (37)$$

$$\overline{\dot{u}^2} \triangleq \frac{1}{\pi}\int_0^\infty \omega^2\left[\Phi_u(\omega) + \frac{1}{T}\,|u_d(j\omega)|^2\right] d\omega \triangleq \text{averaged square control rate} \qquad (38)$$

Disturbance Model

One of the critical assumptions in this study is the selection of the form of the disturbance d(s). The disturbance is assumed to have the form

$$d(t) = Ae^{-at} \qquad (39)$$

The disturbance represents a corrected flow rate change at the diffuser exit. For convenience, d(t) is taken as an equivalent diffuser exit area change (cm^2) instead of corrected flow. A range of parameter a values is considered, from a = 4 to 400 radians per second, so as to account for our uncertainty in establishing the exact nature of the disturbance.

RESULTS

The majority of the results were obtained for a case designated as the reference case, defined as follows:

(1) A single-loop control is used with $H_2 = 0$; H_1 is assumed to be of the following form:

$$H_1(s) = K\left(\frac{b_1}{s} + \frac{b_1}{b_{21}}\right) = K\,\frac{b_1}{s}\left(\frac{s}{b_{21}} + 1\right)$$

which is a proportional-plus-integral (PI) controller. PI control was chosen in view of the results obtained using PI control in previous inlet control programs.

(2) An averaging time T of 1.0 second is assumed.

(3) The disturbance pole a is assumed to be 40 radians per second. Disturbance

amplitude A is assumed to equal 84 square centimeters. This is about the same amplitude that was used in unstart tests reported in reference 5.

Averaged Square Value Comparisons for Reference Case

Reference case designs are compared on the basis of their averaged square values. Three different cases of q_2, r_1, and r_2 cost function penalties are considered. Since the values of q_1, q_2, r_1, and r_2 cannot all be varied independently, q_1 is set to one for all cases. For each case, two of the penalties are set equal to zero and the third is varied from zero to infinity. Thus, although not all combination of penalties are examined, the ones used will give a representative sample of all possible results.

In figure 4(a), the normalized averaged square output rate $\left(\overline{\dot{x}_1^2}\right)_N$ is plotted as a function of normalized averaged square output $\left(\overline{x_1^2}\right)_N$. Quantities $\overline{x_1^2}$ and $\overline{\dot{x}_1^2}$ are normalized with respect to their open-loop values. For each curve, the penalty indicated goes from zero to infinity in the direction of the arrow. The r_1 and r_2 curves go to the open-loop condition for r_1 or r_2 equal ∞. The $q_2 = \infty$ case, which is equivalent to $C = \overline{\dot{x}_1^2}$, appears to also have an open-loop solution, but in fact approaches it quite closely but doesn't reach it. Each of the three curves has a "knee" type characteristic, thus a design trade-off exists between $\left(\overline{\dot{x}_1^2}\right)_N$ and $\left(\overline{x_1^2}\right)_N$. For the q_2 case, for example, one might choose the design having $\left(\overline{\dot{x}^2}\right)_N$ of 1.2 and $\left(\overline{x_1^2}\right)_N$ of 0.5 as one which has a fairly low value of $\left(\overline{x_1^2}\right)_N$ while not having an excessively large value of $\left(\overline{\dot{x}_1^2}\right)_N$. The q_2 curve lies below the r_1 and r_2 curves since it is the only case where $\overline{\dot{x}_1^2}$ is penalized directly.

In selecting a controller design suitable for actual implementation, it is important that the design not require control actuator capabilities beyond those available. Thus, control signal and control rate requirements are examined in figures 4(b) and (c). Here, control and control rate are normalized to their values at the point of minimum $\overline{x_1^2}$ (with $r_1 = r_2 = q_2 = 0$). Figure 4(b) is a plot of normalized averaged square control as a function of $\left(\overline{x_1^2}\right)_N$. For constant $\left(\overline{x_1^2}\right)_N$, as would be expected, the case where u^2 is penalized r_1 results in a controller which requires less $\left(\overline{u^2}\right)_N$ than the other two cases. Similarly in figure 4(c), a plot of $\left(\overline{u^2}\right)_N$ against $\left(\overline{x_1^2}\right)_N$, the r_2 curve falls below the r_1 or q_2 curves. Once the physical limits of control and control rate are known (e.g., for the inlet, bypass door area, and bypass actuator power output) figures

4(b) and (c) can be used in selecting candidate controllers which would not require these physical limits to be exceeded.

Figure 4 can be used in the following manner to assist in coming up with a controller design that minimizes a combination of $\overline{x_1^2}$ and $\overline{\dot{x}_1^2}$ while not causing variables u^2 and $\dot{u}^2$ to exceed limits. First, check to see whether the limits on $\overline{\dot{x}_1^2}$, $\overline{u^2}$, and $\overline{\dot{u}^2}$ are violated for the case $q_2 = r_1 = r_2 = 0$. If the limits are not violated, then this controller is acceptable, being the one of the assumed structure that minimizes $\overline{x_1^2}$ without regard to variables $\overline{\dot{x}_1^2}$, $\overline{u^2}$, and $\overline{\dot{u}^2}$. If one or more of the variables do exceed limits, determine the q_2, r_1, and r_2 values at which the limits are reached ($(q_2)_l$, $(r_1)_l$, and $(r_2)_l$), using figures 4(a), (b), and (c), respectively. Finally go back to the computer and conduct a trial-and-error design using penalty combinations in the ranges $(q_2)_l \leq q_2 \leq \infty$, $(r_1)_l \leq r_1 \leq \infty$, $(r_2)_l \leq r_2 \leq \infty$ until a design is found which minimizes $\overline{x_1^2}$ and does not exceed the limits.

The results displayed in figure 4 can be examined in a conventional manner by displaying the proportional and integral gains of the reference case controller for various values of $\left(\overline{x_1^2}\right)_N$. This is done in figure 5. It can be noted that for constant $\left(\overline{x_1^2}\right)_N$, proportional gain b_1/b_{21} is larger for the r_1 case than for the r_2 case; but integral gain b_1 is higher for the r_2 case than for the r_1 case. That is, proportional gain most directly affects $\overline{\dot{u}^2}$.

Three particular designs are compared on a normalized magnitude frequency response basis in figure 6. Each has a different type of penalty (q_2, r_1, or r_2) but all are for a value of $\left(\overline{x_1^2}\right)_N = 0.4$. The frequency responses displayed are for $G_1(j\omega)G_2(j\omega)$ (open-loop response of x_1 to d) and $G_{c\ell}(j\omega)$ (closed-loop response of x_1 to d). It can be seen that the r_1 design behaves more like a proportional controller in that it attenuates the disturbance similarly at low and high frequency, while the r_2 design acts like an integral controller since it attenuates the disturbance more strongly at low frequencies (less than 10 Hz) than at high. The case where $\overline{\dot{x}_1^2}$ is penalized is a compromise between the other two designs.

Effect of Disturbance Pole Location on Averaged Square Quantities

The effect of having a disturbance which has a pole value a larger than or less than that of the reference case is shown in figure 7. For simplicity, comparisons are made only for the q_2 cases with averaging time T = 1 second. It can be seen that, since the initial value of d(t) is the same for all three cases, the open-loop value of $\overline{x_1^2}$ is largest

for the smallest value of a. Also the case with the largest value of d(t) (a = 400) has the largest value of $\overline{\dot{x}_1^2}$, as would be expected.

Effect of Adding Derivative Control Action and of Using Inner-Loop Controller on Averaged Square Quantities

In an attempt to improve upon the single-outer-loop PI control, two additional configurations were investigated. The first was the addition of derivative action to the outer-loop PI controller. The transfer function for this controller has the form $\frac{Kb_1(s/b_{21}+1)(s/b_{22}+1)}{s(s/5000+1)}$. The second was an inner-loop PI control, which uses signal x_2, the diffuser exit static pressure. One reason for considering use of x_2 instead of x_1 is that x_2 is nearer than x_1 to the point at which the disturbance enters. Thus it might be expected that such a controller could better respond to a diffuser exit disturbance. In figure 8 both of these controllers are compared with the outer-loop PI controller for q_2 designs of the reference case. The outer-loop PI and PID controllers exhibit very similar $\left(\overline{\dot{x}_1^2}\right)_N$ against $\left(\overline{x_1^2}\right)_N$ characteristics. Figure 8(a) shows the PID controller is able to reduce $\left(x_1^2\right)_N$ over that of the PI controller only at large values of $\left(\dot{x}_1^2\right)_N$. The inner-loop PI control is not as effective in reducing $\left(\overline{x_1^2}\right)_N$ as either of the other controllers, except at low values of $\left(\overline{\dot{x}_1^2}\right)_N$. Although there is less phase lag in the loop between x_2 and d than between x_1 and d (see table I); there is also less gain. Consequently, the signal-to-noise ratio at the input to the inner-loop controller ($H_2(s)$) is less than for the outer-loop controller. It is believed that this poorer signal-to-noise ratio accounts for the ineffectiveness of the inner-loop control. It can be noted in figures 8(b) and (c) that $\left(\overline{u^2}\right)_N$ and $\left(\overline{\dot{u}^2}\right)_N$ are essentially identical for the outer-loop PI and PID controllers. Thus, the added complexity of the PID controller hardly seems warranted. Also, the inner-loop PI controller has poorer performance in terms of $\overline{x_1^2}$ and $\overline{\dot{x}_1^2}$, and also in terms of $\left(\overline{u^2}\right)_N$ or $\left(\overline{\dot{u}^2}\right)_N$.

SUMMARY OF RESULTS

This report has demonstrated the use of parameter optimization techniques in the design of controllers for a supersonic inlet. The basic problem formulation allows the

disturbance to be described as a deterministic signal but includes measurements which are corrupted with random noise. The controller design problem was set up as a parameter optimization problem in the time domain but was solved in the frequency domain. A modified conjugate gradient algorithm was used to compute the optimum controller parameters. Control effectiveness was evaluated in terms of average square values of output, output rate, control, and control rate, and also in terms of frequency responses. In applying the method to the inlet, it was found that, of the controllers investigated, proportional-plus-integral (PI) control using throat exit static pressure feedback was most effective. A proportional-plus-integral plus-derivative (PID) controller showed only marginal improvement over the PI control. A PI controller using diffuser exit static pressure was inferior due to signal-to-noise problems. Also investigated was the effect or disturbance dynamic characteristics on controller performance.

Lewis Research Center,
National Aeronautics and Space Administration,
Cleveland, Ohio, July 2, 1974,
501-24.

APPENDIX A

SYMBOLS

A	disturbance amplitude, cm^2
a	disturbance pole, rad/sec
$\underline{b}$	controller parameter vector, $m_p \times 1$
b_1	controller gain, $(rad/sec)^{-m_1}$
b_{2j}	controller poles or zeroes, rad/sec
b_{3j}	controller damping ratio
b_{4j}	controller natural frequency, rad/sec
C	total cost function
C_d	cost function due to deterministic disturbance
$C_{d\infty}$	cost function due to deterministic disturbance with upper limit set equal to ∞
C_v	cost function due to measurement noise
D_q	intermediate variable in cost function
D_r	intermediate variable in cost function
d	disturbance, cm^2
F	cost function integrand or summand
G_a	actuator transfer function, inlet bypass door actuator, cm^2/V
G_{cl}	plant closed-loop transfer function, inlet throat exit static pressure to diffuser exit area disturbance, $(N/cm^2)/cm^2$
G_1	plant transfer function, inlet diffuser exit pressure to diffuser exit disturbance, $N/cm^2/cm^2$
G_2	plant transfer function, inlet throat exit static pressure to diffuser exit static pressure, $N/cm^2/N/cm^2$
H_i	general controller transfer function
H_1	outer-loop controller transfer function, $V/N/cm^2$
H_2	inner-loop controller transfer function, $V/N/cm^2$
j	integer, in eq. (27)
$j\omega$	Fourier transform variable, rad/sec

K^*	measurement gain, pressure transducer gain for inlet, V/N/cm^2
m_p	integer, number of elements in $\underline{b}$ vector
m_1	integer exponent of free s's in controller transfer functions
m_2	integer, number of first-order controller factors
m_3	integer, number of second-order controller factors
N_d	integer, number of frequency points in numerical integration
P_{57}	throat exit static pressure, N/cm^2
P_{87}	diffuser exit static pressure, N/cm^2
$\underline{p}$	transformed parameter vector, $m_p \times 1$
p_{2j}	integer, ± 1
p_{3j}	integer, ± 1
q_1	penalty on output in cost function C
q_2	penalty on output rate in cost function C
r_1	penalty on control in cost function C
r_2	penalty on control rate in cost function C
s	Laplace variable, sec^{-1}
T	deterministic disturbance averaging time, sec
t	time, sec
u	actuator output, inlet bypass door area, cm^2
u_{bp}	bypass door area, cm^2
u_d	component of u due to disturbance
u_v	component of u due to measurement noise
V_q	intermediate variable in cost function
V_r	intermediate variable in cost function
v_1	outer-loop measurement noise, noise on throat exit static pressure measurement, N/cm^2
v_2	inner-loop measurement noise, noise on diffuser exit static pressure measurement, N/cm^2
x_1	plant output, inlet throat exit static pressure, N/cm^2
x_2	plant inner-loop variable, inlet diffuser exit static pressure, N/cm^2

x_{1d} component of x_1 due to disturbance

x_{1v} component of x_1 due to measurement noise

y dummy variable

z dummy variable

Λ diagonal scaling transformation matrix, $m_p \times m_p$

λ element of Λ

τ random noise averaging time, sec

Φ_d power spectral density of d, $(cm^2)^2/Hz$

Φ_u power spectral density of u, $(cm^2)^2/rad/sec$

Φ_v power spectral density of v_1 and v_2, $(N/cm^2)^2/Hz$

Φ_{x1} power spectral density of x_{1v}, $(N/cm^2)^2/Hz$

Φ_y power spectral density of y

Φ_z power spectral density of z

ω frequency, rad/sec

ω_i frequency at i^{th} data point, rad/sec

Subscripts:

$( )_N$ averaged square value of, normalized to averaged square value for reference case with $r_1 = r_2 = q_2 = 0$, $a = 40$, and $T = 1$

$( )_l$ value at which limit is reached

Superscripts:

T matrix transpose

-1 matrix inverse

$\overline{\quad}$ averaged value of

$\cdot$ derivative with respect to time

$*$ complex conjugate

APPENDIX B

COMPUTER PROGRAMS

This appendix describes the FORTRAN IV computer programs which mechanize the controller parameter optimization. The package consists of a main program, two subroutines, and a block data subprogram, written for an IBM 360/67 TSS time sharing computer. The subroutine CGFM conducts the conjugate gradient search. The subroutine CALFG computes the cost function and gradient.

Dimensions

The programs are dimensioned for a maximum number of frequency points N_d of 25 and a maximum number of controller parameters m_p of 10. The vectors dimensioned N_d are AD, A1, A12, DD, DQ, DR, GA, G1G2, HZ, P1, P12, PD, V, VQ, and VR. The vectors dimensioned m_p are B, G, GS, ID, and Z. Vector H has dimension $2m_p$ and vector W has dimension $N_d + 1$.

Main Program

The main program handles data and performs preliminary calculations. The computer variables in the main program are defined in the Main Program Variable List. A flow chart for the main program is presented in figure 9. The following is a FORTRAN listing for the main program:

Main Program Listing

```
C  MAIN PROGRAM FOR CONTROLLER PARAMETER OPTIMIZATION
      COMPLEX G1(25),G1G2(25),GA(25)
      DIMENSION A1(25),A12(25),AD(25),P1(25),P12(25),PD(25),DD(25)
      DIMENSION HZ(25),W(26),V(25),VQ(25),VR(25),DQ(25),DR(25)
      DIMENSION B(10),G(10),ID(10),H(20)
      COMMON/CALC/FDQ,FVQ,FDR,FVR,G1,G1G2,GA,W,VQ,VR,DQ,DR,ID,-
     1 K1,K2,NH1,NH2,INST,NDATA,KNT,GN
      COMMON/ENC/KOUNT,KG
      COMMON/BLOCK/HZ,A1,A12,AD,P1,P12,PD,V,A,AA,T,GA1,GA12,GAD,GK,NP
      LOGICAL KG
      EXTERNAL CALFG
      NAMELIST /NAM3/A,AA,A1,A12,AD,HZ,GA1,GA12,GAD,GK,KPR,-
     1ND,P1,P12,PD,T,V
      NAMELIST /NAM2/K1,K2,NH1,NH2,B,ID,LIMIT,Q1,Q2,R1,R2
```

```
C  PRINT PROGRAM HEADING FOR USER REFERENCE
      WRITE(6,961)
961   FORMAT(' NAM3=(A,AA,A1,A12,AD,HZ,GA1,GA12,GAD,GK,-
     1KPR,ND,P1,P12,PD,T,V)',/-
     2,' NAM2=(K1,K2,NH1,NH2,B,ID,LIMIT,Q1,Q2,R1,R2)'  ,/-
     3,' ID=(1=Z;2=G;3=P;4,5=GZD,GZW;6,7=GPD,GPW)',/-
     4,' INST=(1=SEARCH,2=NAM2,3=NAM3,4=PRINT)',/-
     5,' IER=(0=CONV,1=NOT CONV,2=ERROR)'  )
C  PROMPT,READ AND PRINT NAM3
901   WRITE(6,930)
930   FORMAT(' NAM3?')
      READ(5,NAM3)
      IF(KPR.EQ.1) WRITE(8,NAM3)
C  CONVERSIONS FROM FREQ RESP TO COMPLEX NOS
      NDATA=ND
      GN=GA12
      DO 110 I=1,NDATA
      G1(I)=GA1*A1(I)*CEXP(CMPLX(0.,P1(I)*.0174533))
      G1G2(I)=GA12*A12(I)*CEXP(CMPLX(0.,P12(I)*.0174533))
      W(I)=HZ(I)*6.2831854
      DD(I)=AA**2/(T*(W(I)**2+A**2))
111   GA(I)=GK*GAD*AD(I)*CEXP(CMPLX(0.,PD(I)*.0174533))
      W(NDATA+1)=W(NDATA)
C  PROMPT,READ AND PRINT NAM2
   51 WRITE(6,340)
340   FORMAT(' NAM2?')
      READ(5,NAM2)
      N=NH1+NH2
      WRITE(8,220) K1,K2,NH1,NH2,LIMIT,Q1,Q2,R1,R2,(ID(J),J=1,N)
220   FORMAT(' K1,K2,NH1,NH2,LIMIT=',5I4,/,-
     1' Q1,Q2,R1,R2=',1P4E10.2,' ID=',20I3)
C  COMPUTE VARIABLES IN COST WHICH ARE NOT FUNCTIONS OF B
      DO 210 I=1,ND
      WW=W(I)**2
      GASQ=REAL(GA(I)*CONJG(GA(I)))
      VQ(I)=V(I)*(Q1+WW*Q2)*GASQ
      VR(I)=V(I)*(R1+WW*R2)*GASQ/REAL(G1G2(I)*CONJG(G1G2(I)))
      DQ(I)=DD(I)*(Q1+WW*Q2)
210   DR(I)=DD(I)*(R1+WW*R2)*GASQ
      GO TO 87
C  PROMPT AND READ INST
777   WRITE(6,250)
250   FORMAT(' INST?')
      READ (5,42) INST
42    FORMAT(I1)
      GO TO (28,51,900,35),INST
C  PRINT FREQUENCY RESPONSE HEADING
   35 WRITE (8,41)
41    FORMAT(6X,'HZ',12X,'/Y/',7X,'DEG',11X'REAL       IMAG')
28    SIZE=.1
      EPS=1.E-5
      KNT=0
      ITER=LIMIT*(1-INST/4)
      CALL CGFM(CALFG,N,B,F,G,SIZE,EPS,ITER,IER,H)
C  PRINT SEARCH RESULTS
      WRITE(8,230) F,IER,KNT,KOUNT,SIZE,FDQ,FDR,FVQ,FVR
230   FORMAT(' F=',1PE16.8,'   IER=',I2,'   KNT,KOUNT,SIZE=',-
     1 2I5,E10.3,/,' FDQ,FDR,FVQ,FVR=',1P4E10.3)
```

```
87    WRITE(9,151) (B(J),J=1,")
151   FORMAT(' B=',1P20E11.4)
      GO TO 777
      END
```

Main Program Variable List

A	disturbance time constant a (input variable)
AA	disturbance pulse amplitude (input variable)
AD	$G_a(j\omega)$ normalized, vector (input variable)
A1	$G_1(j\omega)$ normalized, vector (input variable)
A12	$\lvert G_1(j\omega) \cdot G_2(j\omega) \rvert$ normalized, vector (input variable)
B	controller parameter b, vector (input variable). When inputting, those in outer-loop controller transfer function H_1 must precede those in inner-loop transfer function H_2. Damping ratios must precede their natural frequency terms.
CALFG	subroutine (declared external in main program) which computes the cost function and gradient
DD	$\lvert d(j\omega) \rvert^2$, vector
DQ	$D_q(\omega)$, vector
DR	$D_r(\omega)$, vector
EPS	parameter change defining search convergence, for example, 10^{-5}
F	F = C = FDQ + FDR + FVQ + FVR, cost function
FDQ	costs of averaged square output and output rate due to disturbance
FDR	costs of averaged square control and control rate due to disturbance
FVQ	costs of averaged square output and output rate due to measurement noise
FVR	costs of averaged square control and control rate due to measurement noise
G	cost function (scaled) gradient, vector
GA	$G_a(j\omega)$, vector
GAD	gain normalizing AD (input variable)
GA1	gain normalizing A1 (input variable)
GA12	gain normalizing A12 (input variable)
GK	transducer gain K (input variable)

GN	GN = GA12
G1	$G_1(j\omega)$, vector
G1G2	$G_1(j\omega) \cdot G_2(j\omega)$, vector
H	storage, vector
HZ	frequency in hertz, vector (input variable)
I	index of element in vector, integer
ID	integer vector which identifies corresponding parameter in B as to type (input variable). 1 = zero, 2 = gain, 3 = pole, 4 = complex zero damping, 5 = complex zero natural frequency, 6 = complex pole damping, 7 = complex pole natural frequency.
IER	search convergence parameter. 0 = convergence to EPS in LIMIT; 1 = convergence to EPS in LIMIT not obtained; 2 = probable error occurred.
INST	branching instruction parameter (input variable). 1 = search for optimum; 2 = return to NAM2 namelist; 3 = return to NAM3 namelist; 4 = print frequency, system closed-loop frequency response (normalized by GN), and system Nyquist plot.
ITER	set equal to LIMIT except for INST = 4 case when ITER = 0.
J	index of element in vector
KG	logical variable .TRUE. means compute gradient
KNT	count of cost function evaluations
KOUNT	count of line search iterations
KPR	if equal to 1 causes NAM3 variables to be printed (input variable)
K1	exponent of free s in H1 (input variable)
K2	exponent of free s in H2 (input variable)
LIMIT	maximum number of iterations (input variable)
N	NH1 + NH2
ND	number of frequency points over which integration is performed N_d
NDATA	NDATA = ND
NH1	number of parameters of B in H1 (input variable)
NH2	number of parameters of B in H2 (input variable)
PD	$G_a(j\omega)$ in degrees, vector (input variable)

P1	$\angle G_1(j\omega)$ in degrees, vector (input variable)
P12	$\angle G_1(j\omega) \cdot G_2(j\omega)$ in degrees, vector (input variable)
Q1	q_1 (input variable)
Q2	q_2 (input variable)
R1	r_1 (input variable)
R2	r_2 (input variable)
SIZE	parameter step size; for example, set to 0.1 at start of search
T	T (input variable)
V	$\Phi_v(\omega)$, vector (input variable)
VQ	$V_q(\omega)$, vector
VR	$V_r(\omega)$, vector
W	radian frequency ω, vector
WW	frequency squared

Program Input and Output

The program starts by printing a heading referencing the namelist variables and variable codes. Then the program prompts for NAM3 namelist data. The namelist variables are entered according to the FORTRAN rules for namelist data. The NAM3 variables are A, AA, A1, A12, AD, HZ, GA1, GA12, GAD, GK, KPR, ND, P1, P12, PD, T, and V. Since eight of the variables are vectors, the input could be lengthy. Thus, an alternative to entering NAM3 data at run time is to use the block data subprogram. The following is a listing of the subprogram for the inlet investigated in the report:

```
 BLOCK DATA
 COMMON/BLOCK/HZ,A1,A12,AD,P1,P12,PD,V,A,AA,T,GA1,GA12,GAD,GK,ND
 REAL HZ(25)/.001,1.,3.,7.,10.,15.,20.,25.,30.,40.,50.,60.,70.,-
1  80.,90.,100.,110.,120.,130.,140.,150.,300.,3*600./
 REAL A1(25)/1.,1.,1.,.997,.927,.818,.732,.643,.565,.411,.359,.326,-
1  .318,.397,.465,.486,.46,.407,.326,.303,.209,.042,3*.0093/
 REAL A12(25)/1.,1.,.95,.774,.697,.671,.628,.602,.53,.437,.347,.313,-
1    .334,.352,.318,.322,.299,.288,.27,.26,.237,.012,3*.0013/
 REAL AD(25)/1.,1.,.999,1.,.996,.993,.997,.996,1.,1.012,1.016,1.012,-
1  1.01,1.011,1.005,1.024,.954,.908,.782,.689,.609,.051,3*.0063/
 REAL P1(25)/0.,-1.,-8.,-18.,-26.,-39.,-46.,-51.,-58.,-63.,-62.,-55.,-
1  -40.,-55.,-65.,-74.,-94.,-110.,-125.,-115.,-18.,-174.,3*-178./
 REAL P12(25)/0.,-2.,-13.,-24.,-31.,-35.,-44.,-57.,-62.,-75.,-87.,-90.,-
1-92.,-105.,-119.,-128.,-145.,-156.,-166.,-172.,-177.,-251.,3*-266./
```

```
 REAL PD(25)/0.,-2.,-5.,-10.,-13.,-18.,-23.,-27.,-32.,-42.,-51.,-59.-
1,-68.,-77.,-85.,-96.,-116.,-128.,-146.,-160.,-173.,-226.,3*-250./
 REAL V(25)/.24E-5,4*2.4E-5,4.E-5,2*5.7E-5,7.E-5,6.E-5,4.4E-5,-
1  7.E-5,3.4E-5,4*4.E-5,3*3.3E-5,4.4E-5,7.E-5,3*4.E-5/
 DATA T,1,AA/1.,40.,84./
 DATA UD,GA1,GA12,GAD,GK/23,.01E,.02502,36.9,.762/
 END
```

The NAM3 variables are printed if KPR is set to one. Then the program prompts for NAM2 namelist data. The NAM2 variables are B, ID, K1, K2, LIMIT, NH1, NH2, Q1, Q2, R1, and R2. Then the NAM2 variables are printed and a prompt for the INST variable is printed.

The INST variable is entered in I1 format. The INST code values are 1, 2, 3, and 4. Making INST = 1 causes a search for the optimum parameters. After the search results are printed, another INST prompt is issued. Making INST = 2 returns the program to request NAM2. Making INST = 3 returns the program to request NAM3. Making INST = 4 causes the system frequency response to be printed. The frequency is printed under HZ. The system closed-loop frequency response normalized magnitude is printed under /Y/ and phase in degrees under DEG. The real part of the system open-loop transfer function is printed under REAL and the imaginary part under IMAG. Then the zero iteration search results are printed, and another INST prompt is issued.

Subroutine CALFG(N, E, F, G)

The purpose of this subroutine is to compute the cost function and its gradient. The CALFG program variables are defined in the CALFG Program Variable List. Those variables in the common blocks and subroutine call are labeled the same as those in the main program and are not repeated again.

The Data statement IN and RSNAT values are variables in the variable step size integration. Smaller step sizes are taken near a system resonance; that is, when the absolute value squared of the denominator of the system closed-loop transfer function $|1. + \text{OPEN}|^2$, is less than RSNAT. The variable IN is the number of subintervals into which an interval is divided. Upon detecting a resonance, the program fills in extra points starting from the previous frequency by linear interpolation, using data from the present and past frequency points. A flow chart of the integration logic for the subroutine CALFG is given in figure 10.

FORTRAN Listing of Subroutine CALFG

```
      SUBROUTINE CALFG(N,B,F,G)
      COMPLEX Z(10),GA(25),G1(25),G1G2(25)
      COMPLEX Y,GF,GT,H1,H2,S,OPEN,G11,G1G21,GA1,H2G211
      DIMENSION W(26),VR(25),VO(25),DO(25),DR(25)
      DIMENSION GS(10),ID(10),B(1),G(1)
      COMMON/CALC/EDO,EVO,EDR,EVR,G1,G1G2,GA,W,VO,VR,DO,DR,ID,-
     1 K1,K2,NH1,NH2,INST,NDATA,KNT,GN
      COMMON/EVC/KOUNT,KG
      LOGICAL KG,RSNT
      DATA RSNAT,IN/.5,3/
C  INITIALIZATIONS
      KNT=KNT+1
      RSNT=.TRUE.
      DO 70 J=1,N
70    G(J)=0.
80    H1=CMPLX(0.,0.)
      H2=CMPLX(0.,0.)
      EDO=0.
      EVO=0.
      EDR=0.
      EVR=0.
      WS=W(1)
      IDXN=IN
      R=1./FLOAT(IN)
C  INDEX I FOR EACH OPEN LOOP DATA POINT; PROVIDE
C  FOR INTERPOLATION BETWEEN POINTS IN RESONANCE
      DO 200 I=1,NDATA
90    IDX=IDXN
100   RI=FLOAT(IDX)*R
      RIN=1.-RI
      WI=W(I-1)*RIN+W(I)*RI
      S=CMPLX(0.,WI)
C  BUILD CONTROLLERS H1 AND H2
      IF(NH1.GT.0) H1=S**K1
      IF(NH2.GT.0) H2=S**K2
      DO 10 J=1,N
      IDJ=ID(J)
      GO TO (1,3,1,2,10,2,10),IDJ
1     ST=(S/B(J)+1.)**(2-IDJ)
      IF(KG) Z(J)=S/(S+B(J))*(FLOAT(IDJ)-2.)
      GO TO 8
2     ST=(S/B(J+1))**2+2.*S*B(J)/B(J+1)+1.
      IF(.NOT.KG) GO TO 88
      Z(J)=2.*S*B(J)/(B(J+1)*ST)*(5.-FLOAT(IDJ))
      Z(J+1)=-Z(J)*(1.+S/(B(J)+B(J+1)))
88    ST=ST**(5-IDJ)
      GO TO 8
3     ST=B(J)
      Z(J)=CMPLX(1.,0.)
8     IF(J.LE.NH1) H1=H1*ST
      IF(J.GT.NH1) H2=H2*ST
10    CONTINUE
C  CHECK FOR RESONANCE; COMPUTE SYSTEM COSTS
      GA1=GA(I-1)*RIN+GA(I)*RI
      G11=G1(I-1)*RIN+G1(I)*RI
      G1G21=G1G2(I-1)*RIN+G1G2(I)*RI
```

```
      OPEN=GAI*(G11*H2+G1G21*H1)
      IF(IDX.LT.IN) GO TO 110
      IF(REAL((1.+OPEN)*CONJG(1.+OPEN)).LT.RSNAT) GO TO 120
      WP1=W(I+1)
      IDXN=IN
      RSNT=.FALSE.
      GO TO 140
110   WP1=(W(I)*FLOAT(IDX+1)+W(I-1)*FLOAT(IN-IDX-1))*R
      GO TO 140
120   IDXN=I
      IF(RSNT) GO TO 130
      IF(I.GT.2) WSS=W(I-2)
      IF(I.EQ.2) WSS=W(1)
      CRCT=-1.+((W(I)+FLOAT(IN-I)*W(I-1))*R-WSS)/(W(I)-WSS)
      EDO=EDO+CRCT*DOW
      EVO=EVO+CRCT*VOW*HMAG
      EDR=EDR+CRCT*DRW*HM
      EVR=EVR+CRCT*VRW*HMAG
      DO 125 J=1,N
125   G(J)=G(J)+CRCT*GS(J)
      RSNT=.TRUE.
      GO TO 90
130   WP1=W(I)*(1.-R)+W(I+1)*R
140   Y=G1G21/(1.+OPEN)
      YY=REAL(Y*CONJG(Y))*(WP1-WS)
      H2G21=(G11*H2)/G1G21+H1
      DOW=(RI*DO(I)+RIM*DO(I-1))*YY
      VOW=(RI*VO(I)+RIM*VO(I-1))*YY
      VRW=(RI*VR(I)+RIM*VR(I-1))*YY
      DRW=(RI*DR(I)+RIM*DR(I-1))*YY
      HMAG=REAL(H1*CONJG(H1)+H2*CONJG(H2))
      HM=REAL(H2G21*CONJG(H2G21))
      EDO=EDO+DOW
      EDR=EDR+DRW*HM
      EVO=EVO+VOW*HMAG
      EVR=EVR+VRW*HMAG
      IF(.NOT.KG) GO TO 180
C  COMPUTE GRADIENT
      ST=(DOW+HMAG*(VOW+VRW)+DRW*HM)*CONJG(-Y*GAI)+DRW*H2G21
      DO 160 J=1,N
      IF(J.EQ.1) GF=(ST+(VOW+VRW)*H1)*CONJG(H1)
      IF(J.EQ.NH1+1) GF=(ST*CONJG(G11/G1G21)+(VOW+VRW)*H2)*CONJG(H2)
      GS(J)=REAL(GF*CONJG(Z(J)))
160   G(J)=G(J)+GS(J)
180   IF(INST.LT.4) GO TO 190
C  PRINT SYSTEM FREQUENCY RESPONSE AND OPEN LOOP
      HZ=WI/6.2831854
      YMAG=CABS(Y/GN)
      DEG=ATAN2(AIMAG(Y),REAL(Y))*57.29578
      WRITE(8,300) HZ,YMAG,DEG,OPEN
190   IDX=IDX+1
      WS=WI
      IF(IDX.LE.IN) GO TO 100
200   CONTINUE
      E=EDO+EVO+EDR+EVR
      RETURN
300   FORMAT(1PE10.3,2(5X,2E10.3))
      END
```

If the user desired to use a search routine other than subroutine CGFM, the scaled gradient $\Delta VC(b)$ may not be desired. In such a case the unscaled gradient may be obtained by dividing each term in the gradient vector by its corresponding parameter in the $\underline{b}$ vector.

CALFG Program Variable List

DEG	$\angle G_{c\ell}(j\omega)$ in degrees
DQW	partial product
DRW	partial product
GF	gradient of F
GS	saved gradient partial sum, vector
G1I	$G_1(j\omega)$ value
G1G2I	$G_1(j\omega) \cdot G_2(j\omega)$ value
HM	temporary value
HMAG	temporary value
H2G2II	temporary value H2/G2 + H1
HZ	frequency value
H1	H_1
H2	H_2
I	frequency index
IDJ	ID(J) value
IDX	counter for data insertions
IDXN	counter value for logic
IN	number of subintervals inserted into an interval near a system resonance; for example, IN = 3 means each interval is divided into thirds
J	parameter index
OPEN	$G_a \cdot G_1(H_2 + G_2H_1)$
R, RI, RIM	temporary values
RSNAT	condition defining existence of system resonance for $\lvert 1 + \text{OPEN} \rvert^2 <$ RSNAT, that is, for RSNAT = 0.5. The closed-loop frequency response magnitude is $\cdot 1.42 = (1/\sqrt{0.5})$ times its open-loop value.

RSNT	temporary logic; true = resonance
S	s
ST	temporary value
VQW	intermediate product
VRW	intermediate product
WI	ω value
WP1	next frequency
WS	saved WI
WSS	saved WS
Y	$G_{cl}(j\omega)$
YMAG	$\|G_{cl}(j\omega)\|$, GA12
YY	partial product
Z	partial product in controller gradient, vector

Subroutine CGFM(CALFG, N, B, F, G, SIZE, EPS, ITER, IER, H)

The purpose of Subroutine CGFM is to perform the conjugate gradient search function minimization. Several nonstandard modifications relative to the conjugate gradient search described in reference 6 exist in the CGFM subroutine. The gradient is the scaled gradient $\Lambda\nabla C(\underline{b})$ and every iteration updated $\underline{b}$ parameters change the scaled coordinate system. This simplifies calculations somewhat but violates theoretical convergence arguments for quadratic sosts. However, away from the minimum point, $C(\underline{b})$ may be quite nonquadratic; and around the minimum, changes in scaling are generally small. This, it is believed, accounts for the decreased convergence times obtained using the scaling modification. Another nonstandard modification to the search is that the signs of the parameters $\underline{b}$ are not allowed to change during the search. This prevents formation of an unstable controller during the search.

The CGFM program variables are defined in the CGFM Program Variable List. Variables carried over in the common block and subroutine call are labeled the same as those described in the main program and are not repeated again. Figure 11 is a flow chart of CGFM.

```
      SUBROUTINE CGFM(CALFG,N,B,F,G,SIZE,EPS,ITER,IER,H)
      DIMENSION B(1),H(1),G(1)
      LOGICAL KG
      COMMON/FMC/KOUNT,KG
C  INITIALIZATIONS
      KOUNT=0
      STEP=2.
      IER=-5
    5 BETA=0.
      NCYC=0
   15 K=0
      DO 20 J=1,N
   20 H(J)=B(J)
      KG=.TRUE.
      CALL CALFG(N,B,F,G)
C  TEST FOR STOPPING SEARCH
      IF(KOUNT.GE.ITER) IER=1
      IF(SIZE.LT.EPS) IER=0
   40 IF(IER.GT.-2) RETURN
C  COMPUTE PAST GRADIENT WEIGHTING
      TSQR=0.
      DO 50 J=1,N
   50 TSQR=TSQR+G(J)**2
      IF(NCYC.EQ.0) GO TO 60
      BETA=TSQR/TSAVE
   60 SCALE=0.
      DO 70 J=1,N
      JN=J+N
      H(JN)=-G(J)+BETA*H(JN)
   70 SCALE=SCALE+ABS(H(JN))
      IF(SCALE.GT.0.) GO TO 80
      IER=0
      GO TO 40
   80 SCALE=SIZE/SCALE
      TSAVE=TSQR
      NCYC=NCYC+1
      FSS=F
      L=1
C  UPDATE B'S
  100 DO 110 J=1,N
      JN=J+N
  110 B(J)=H(J)+ABS(1.+SCALE*H(JN))
      FS=F
      KG=.FALSE.
      CALL CALFG(N,B,F,G)
C  LOGIC CHANGES LINE SEARCH STEP SIZE OR CONCLUDES SEARCH
      IF(K.GT.0) GO TO 120
      IF(F.LT.FS) GO TO 130
      IF(L.GT.1) GO TO 140
      GO TO 150
  120 IF(F.LT.FSS) GO TO 140
      GO TO 160
  130 SCASV = SCALE
      L= L+1
      SCALE= SCALE*STEP
```

```
      FSS=FS
      IF(L.LT.15) GO TO 100
      IER=2
      GO TO 40
C  FIT QUADRATIC CURVE TO 3 PTS. BRACKETING LINE SEARCH MIN.
140   DO 148 J=1,N
      JN=J+N
      R1=H(J)
      R2=H(J)*ABS(1.+SCASV*H(JN))
      R3=B(J)
      IF(L.GT.3) R1=R1+(R2-R1)/STEP
      X1=(FSS-FS)*(R1-R3)
      X2=(FSS-F)*(R2-R1)
      IF(ABS(R2-R3).GT.EPS/4.) GO TO 147
      IF(L.GT.1) B(J)=R2
      GO TO 148
147   B(J)=(X1*(R1+R3)+X2*(R1+R2))/((X1+X2)*2.)
148   IF(B(J)*H(J).LE.0.) B(J)=-.1*B(J)+EPS*R3
C  UPDATE SEARCH VARIABLES
      SIZE=SIZE*(FLOAT(L)+2.)/4.
      KOUNT=KOUNT+1
      IF(NCYC.GT.N) GO TO 5
      GO TO 15
  150 SCASV= SCALE
      SCALE= SCALE/(1.+STEP)
      K= K+1
      SIZE= SIZE/(1.+STEP)
      GO TO 100
  160 SIZE= SIZE/(1.+STEP)
      DO 180 J=1,N
  180 B(J)=H(J)
      GO TO 5
      END
```

CGFM Program Variable List

BETA	conjugate direction weighting
FS	saved F
FSS	saved FS
J	parameter index
JN	J + N
K	indicator for step size reductions
L	number step size increases within iteration
NCYC	number of iterations before restarting conjugate search
R1, R2, R3	terms in quadratic curve fit
SCALE	step size scale factor

SCASV	saved SCALE
STEP	step size
TSAVE	saved TSQR
TSQR	squared gradient terms sum
X1, X2	partial product

APPENDIX C

SAMPLE PROBLEM

A sample problem, using the inlet data from table I, is presented. The following is a computer terminal printout of the problem solution:

```
1    NAM3=(A,AA,A1,A12,AD,HZ,GA1,GA12,GAD,GK,KPR,MD,P1,P12,PD,T,V)
2    NAM2=(K1,K2,NH1,NH2,B,ID,LIMIT,Q1,Q2,R1,R2)
3    ID=(1=Z;2=Q;3=P;4,5=CZD,CZW;6,7=CPD,CPW)
4    INST=(1=SEARCH,2=NAM2,3=NAM3,4=PRINT)
5    IER=(0=CONV,1=NOT CONV,2=ERROR)
6    NAM3?
7*    &nam3 &end
8    NAM2?
9*    &nam2 k1=-1,nh1=2,b=10,10000,ID=2,1,limit=50,
10*   q1=1,q2=.0001,r1=0,r2=0,k2=0,nh2=0 &end
11   K1,K2,NH1,NH2,LIMIT=  -1    0    2    0   50
12   Q1,Q2,R1,R2=  1.00E 00  1.00E-04  0.00       0.00      ID=  2  1
13   B= 1.0000E 01 1.0000E 04
14   INST?
15*  1
16   F=  3.11901510E-01   IER= 0   KNT,KOUNT,SIZE=  102    24 1.301E-06
17   FDO,FDR,FVQ,FVP= 2.884E-01 0.000      2.352E-02 0.000
18   B= 4.7216E 01 1.3056E 02
19   INST?
20*  4
21        HZ            /Y/          DEG          REAL         IMAG
22   1.000E-03     1.831E-04 8.999E 01      2.629E-01-5.462E 03
23   1.000E 00     1.906E-01 7.884E 01     -1.189E-01-5.467E 00
24   3.000E 00     5.111E-01 5.477E 01     -2.967E-01-1.720E 00
25   7.000E 00     7.489E-01 1.248E 01     -1.690E-01-6.145E-01
26   1.000E 01     7.295E-01-6.281E 00     -1.321E-01-3.995E-01
27   1.500E 01     7.023E-01-1.759E 01     -9.836E-02-2.859E-01
28   2.000E 01     6.732E-01-3.047E 01     -9.300E-02-2.183E-01
29   2.500E 01     6.671E-01-4.611E 01     -1.138E-01-1.704E-01
30   3.000E 01     5.864E-01-5.359E 01     -1.060E-01-1.322E-01
31   4.000E 01     4.974E-01-7.013E 01     -1.066E-01-7.616E-02
32   5.000E 01     3.830E-01-9.489E 01     -9.464E-02-3.339E-02
33   6.000E 01     3.425E-01-8.886E 01     -8.622E-02-1.817E-02
34   7.000E 01     3.680E-01-9.165E 01     -9.233E-02-5.503E-03
35   8.000E 01     3.878E-01-1.067E 02     -9.264E-02 2.755E-02
36   9.000E 01     3.410E-01-1.222E 02     -8.885E-02 5.180E-02
37   1.000E 02     3.379E-01-1.324E 02     -8.084E-02 7.316E-02
38   1.100E 02     2.975E-01-1.404E 02      2.260E-03 7.627E-02
39   1.200E 02     2.796E-01-1.500E 02      2.819E-02 6.382E-02
40   1.300E 02     2.585E-01-1.670E 02      4.373E-02 3.531E-02
41   1.400E 02     2.488E-01-1.720E 02      4.486E-02 1.504E-02
42   1.500E 02     2.283E-01-1.771E 02      3.927E-02 1.412E-03
43   3.000E 02     1.200E-02 1.000E 02     -9.206E-05-1.383E-04
44   6.000E 02     1.300E-03 9.400E 01     -1.007E-06-9.075E-07
45   F=  3.11901510E-01   IER= 1   KNT,KOUNT,SIZE=    1     0 1.000E-01
46   FDO,FDR,FVQ,FVP= 2.884E-01 0.000      2.352E-02 0.000
47   B= 4.7216E 01 1.3056E 02
48   INST?
```

*User input.

Responses in capital letters are program output (43 lines), and lower case letters are user input (5 starred lines). The line numbers to the left of each line were added for discussion purposes. The listing shows the problem of optimizing a two-parameter controller for a given cost function. The controller was a single-loop proportional plus integral controller with the form $H_2(s) = 0$ and $H_1(s)/K = b_1(s/b_{21} + 1)/s = (b_1/s) + (b_1/b_{21})$. The cost function was $C = \overline{x_1^2} + 0.0001\ \overline{\dot{x}_1^2}$. It penalizes system output and output rate but not control or control rate.

Lines 1 to 5 were printed by the computer after the user called the program. These lines list the NAM3 and NAM2 variables and parameters ID, INST, and IER. At line 6, the computer prompted for NAM3 namelist. In line 7 the user signed in and out of the namelist without updating any values from the block data subprogram. Since KPR $\neq$ 1, there is no print of the NAM3 variables. In line 8 the computer prompted for NAM2. In lines 9 and 10 the user supplied NAM2 input. The initial parameter estimates were $b_1 = 10$ and $b_{21} = 1000$. The transducer gain K is part of the NAM3 input and not input here. In lines 11 to 13, the computer outputed the updated NAM2 values, and in line 14 it prompted for an INST input.

In line 15 the user entered a 1 to search for the optimum controller parameters. Lines 16 to 18 list the search results. The cost function F was 0.3119. IER = 0 meant that the (scaled) parameters were changing less than EPS (1.E-5) as can be verified noting that SIZE was 1.39 E-6. The iteration line search count KOUNT was 24, and the number of cost function evaluations KNT was 102. The q_1 and q_2 costs due to the disturbance, FDQ, was 0.2884 and due to the noise, FVQ, was 0.0235. FDR and FVR costs were zero because r_1 and r_2 were zero. The optimum parameters $b_1 = 47$ and $b_{21} = 131$ were returned.

At line 19 the computer prompted for another INST input. The user input INST = 4 in line 20, which directed the program to display the system frequency response. Line 21 contains the column headings for the data given in lines 22 to 44. The first frequency was made 0.001 instead of zero (in NAM3) because $H_1(s)$ would be infinite at zero. A system stability spot check can be performed using the Nyquist criteria and the open-loop REAL and IMAG data by reading the IMAG column until a sign change occurs in which the REAL part is negative (between IMAG = -0.0056 and +0.028). A stability check is that the REAL part is greater than -1.0; -0.09 is. A complete test may not always be so simple but for this problem the response sim.ply spirals into zero.

Lines 45 to 47 repeat the list of costs and search parameters, and at line 48 the computer prompted for another INST input.

This example problem is also used to study convergence and parameter scaling. In figure 12 the cost function contours are plotted as functions of b_1 and b_{21}. The contours form an elongated valley more sensitive to b_1 than to b_{21} and thus not well scaled away from the minimum. The search trajectory starting at (10, 10 000) is also

shown. The search run in figure 12 took 3.5 seconds central processor unit time on the IBM 360/67 TSS. The same problem was run using a standard conjugate gradient search for two different but constant scaling rules. One rule scaled the parameters by their initial estimates (10, 10 000). The problem ran about the same time, but it converged to a slightly less accurate $F = 0.3121$ instead of 0.3119. The other rule was to scale the parameters near the solution (40, 130). In this case thesearch could not advance significantly from the initial point for b_{12} which remained at 10 000 while b_1 moved to 46.

REFERENCES

1. Neiner, George H.; Crosby, Michael J.; and Cole, Gary L.: Experimental and Analytical Investigation of Fast Normal Shock Position Controls for a Mach 2.5 Mixed-Compression Inlet. NASA TN D-6382, 1971.

2. Lehtinen, Bruce; and Zeller, John R.: Application of Quadratic Optimization to Supersonic Inlet Control. IFAC J. -Automatica, vol. 8, no. 5, Sept. 1972. pp. 563-574.

3 Zeller, John R.; Lehtinen, Bruce; Geyser, Lucille C.; and Batterton, Peter G.: Analytical and Experimental Performance of Optimal Controller Designs for a Supersonic Inlet. NASA TN D-7188, 1973.

4 Stefani, R. T.; Dial, J. H.; Williams, T. L.; and Silverstone, D. E.: Control System Design Using Optimization Techniques. University of Arizona, (NASACR-109405), 1969.

5. Cole, Gary L.; Neiner, George H.; and Baumbick, Robert J.: Terminal-Shock Position and Restart Control of a Mach 2.7, Two-Dimensional, Twin-Duct, Mixed-Compression Inlet. NASA TM X-2818, 1973.

6. Fletcher, R.; and Reeves, C. M.: Function Minimization by Conjugate Gradients. Computer J., vol. 7, no. 2, Jul. 1964. pp. 149-154.

7. Cooper, George R.; and McGillem, Clare D.: Methods of Signal and System Analysis. Holt, Rinehart, and Winston, Inc., 1967.

8. Baumbick, Robert J.; Neiner, George H.; and Cole, Gary L.: Experimental Dynamic Response of a Two-Dimensional, Mach 2.7, Mixed-Compression Inlet. NASA TN D-6957, 1972.

TABLE I. - MIXED COMPRESSION INLET AND BYPASS DOOR FREQUENCY RESPONSE DATA AND MEASUREMENT NOISE POWER SPECTRAL DENSITY (PSD)

Frequency, Hz	Inlet frequency response				Bypass door frequency response bypass door area to command voltage, $G_a(j\omega)$		Measurement noise PSD, $\Phi_v(\omega)$, $\frac{(N\ cm^{-2})^2}{rad\ sec}$
	Diffuser exit static pressure to bypass door area $G_1(j\omega)$		Throat exit static pressure to bypass door area $G_1(j\omega)G_2(j\omega)$				
	Magnitude, $\frac{0.016\ N\ cm^2}{cm^2}$	Phase, deg	Magnitude, $\frac{0.026\ N\ cm^2}{cm^2}$	Phase, deg	Magnitude, $\frac{36.8}{cm^2\ V}$	Phase, deg	
0.001	1	0	1	0	1	0	$0.024 \cdot 10^{-5}$
1	1	-1	1	-2	1	-2	$.24 \cdot 10^{-4}$
3	1	-8	.95	-13	1	-5	$.24 \cdot 10^{-4}$
7	1	-18	.77	-24	1	-10	$.24 \cdot 10^{-4}$
10	.93	-26	.70	-31	1	-13	$.24 \cdot 10^{-4}$
15	.82	-39	.67	-35	.99	-18	$.40 \cdot 10^{-4}$
20	.73	-46	.63	-44	1	-23	$.57 \cdot 10^{-4}$
25	.64	-51	.60	-57	1	-27	$.57 \cdot 10^{-4}$
30	.56	-58	.53	-62	1	-32	$.70 \cdot 10^{-4}$
40	.41	-63	.44	-75	1.01	-42	$.80 \cdot 10^{-4}$
50	.36	-62	.35	-87	1.02	-51	$.44 \cdot 10^{-4}$
60	.33	-55	.31	-90	1.01	-59	$.70 \cdot 10^{-4}$
70	.32	-49	.33	-92	1.01	-68	$.54 \cdot 10^{-4}$
80	.39	-55	.35	-105	1.01	-77	$.40 \cdot 10^{-4}$
90	.46	-65	.32	-119	1.0	-85	$.40 \cdot 10^{-4}$
100	.49	-74	.32	-128	1.02	-96	$.40 \cdot 10^{-4}$
110	.46	-94	.30	-145	.95	-116	$.40 \cdot 10^{-4}$
120	.41	-110	.29	-156	.91	-128	$.33 \cdot 10^{-4}$
130	.33	-125	.27	-166	.78	-146	$.33 \cdot 10^{-4}$
140	.30	-115	.26	-172	.69	-160	$.33 \cdot 10^{-4}$
150	.21	-98	.24	-177	.61	-173	$.44 \cdot 10^{-4}$
300	.042	-174	.012	-251	.051	-226	$.70 \cdot 10^{-4}$
600	.0093	-178	.0013	-266	.0063	-250	$.40 \cdot 10^{-4}$

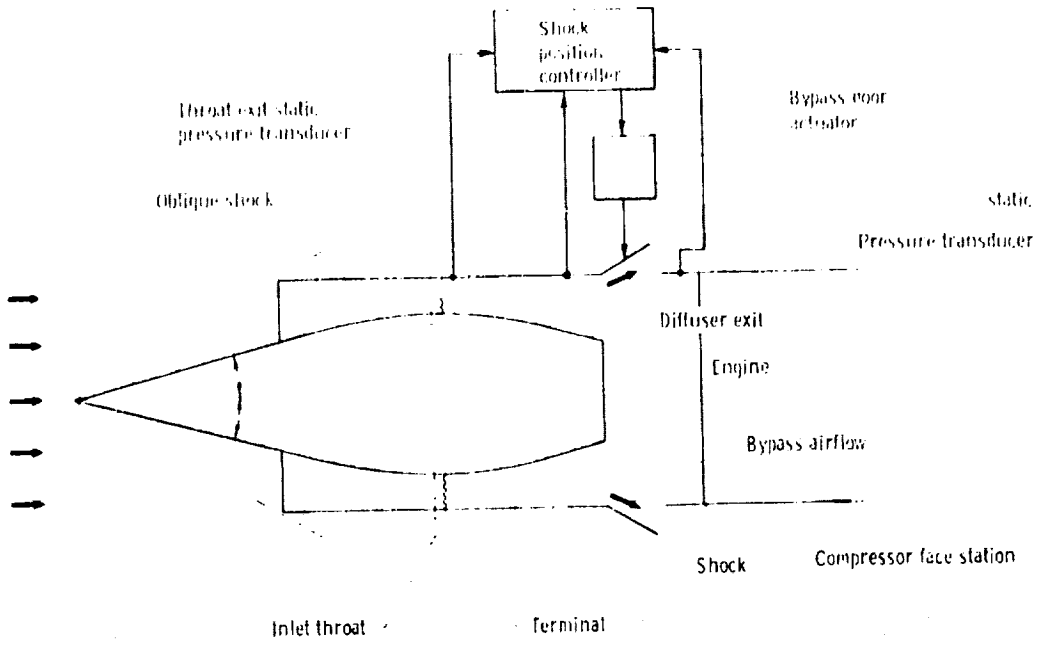

Figure 1. - Schematic of mixed compression inlet with terminal shock position control.

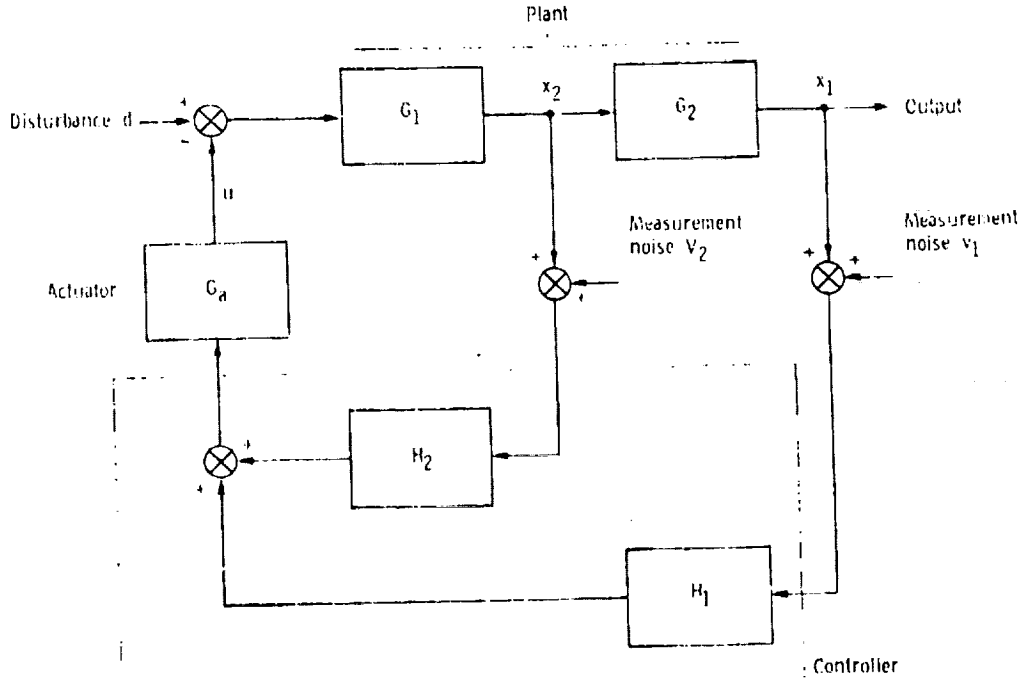

Figure 2. - General control system block diagram.

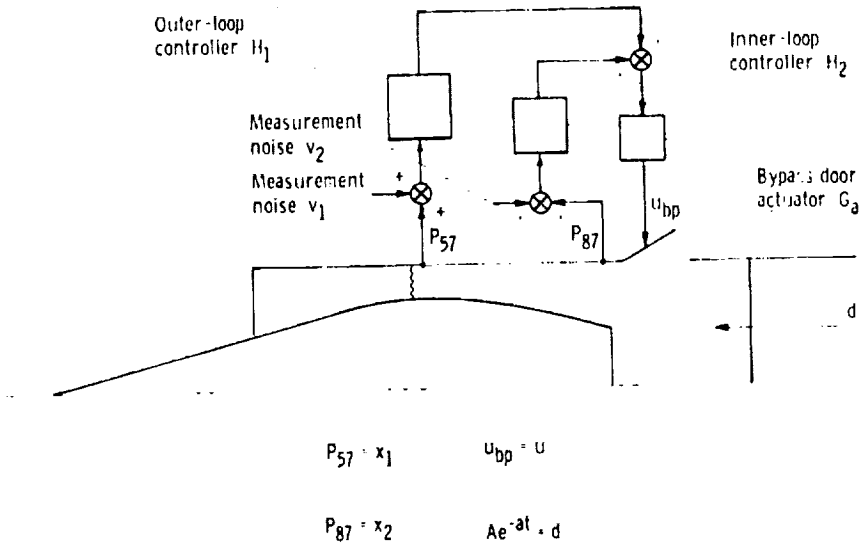

Figure 3. - Inlet control system block diagram.

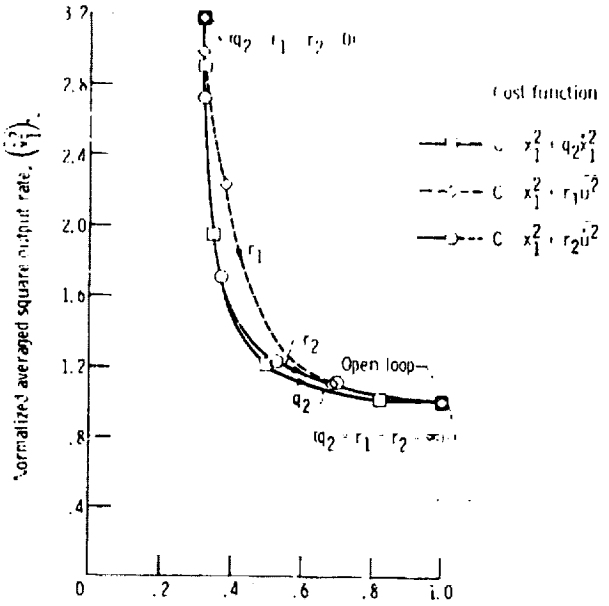

(a) Output rate as function of output.

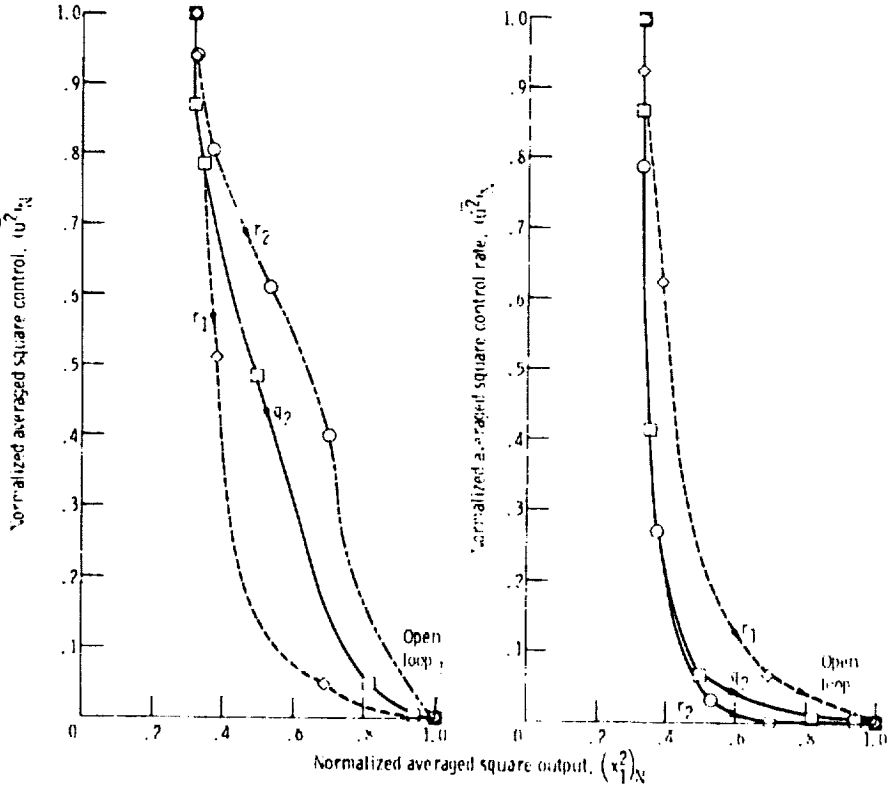

(b) Control as function of output.

(c) Control rate as function of output.

Figure 4. Normalized averaged square output rate, control and control rates as functions of normalized averaged square output as q_2, r_1, and r_2 penalties vary from 0 to ∞; reference case

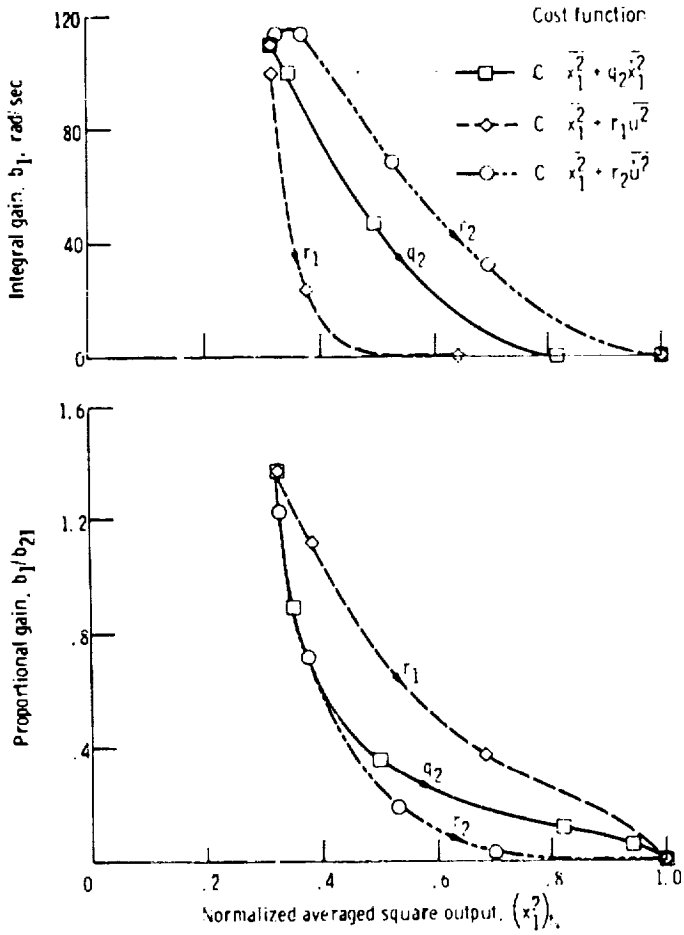

Figure 5. - Proportional and integral gains as function of normalized averaged square output as q_2, r_1, and r_2 penalties vary from 0 to ∞; reference case.

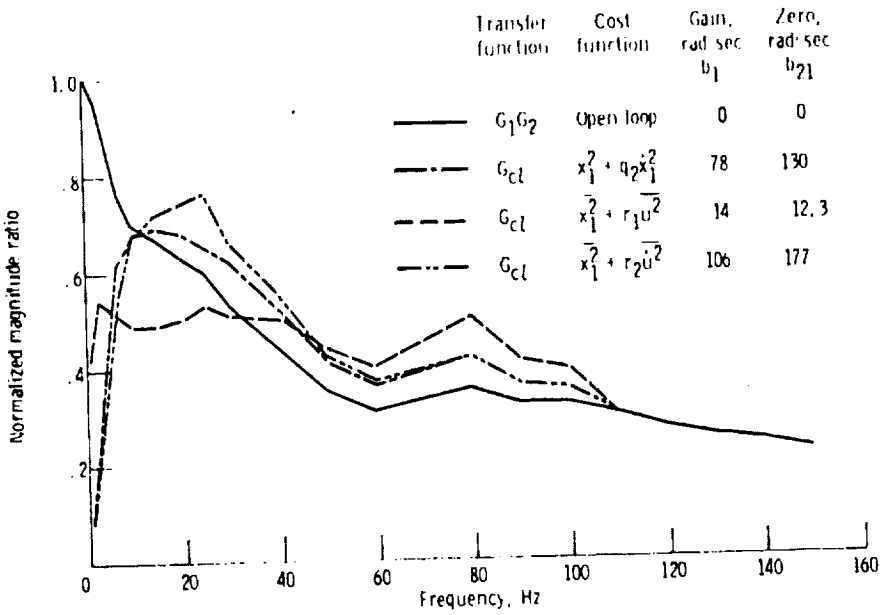

Figure 6. - Frequency response of output $x_1(j\omega)$ in response to disturbance $d(j\omega)$; normalized to magnitude of open loop response at 1 hertz; reference case; $\left(\overline{x_1^2}\right)_N = 0.4$ for all closed-loop cases.

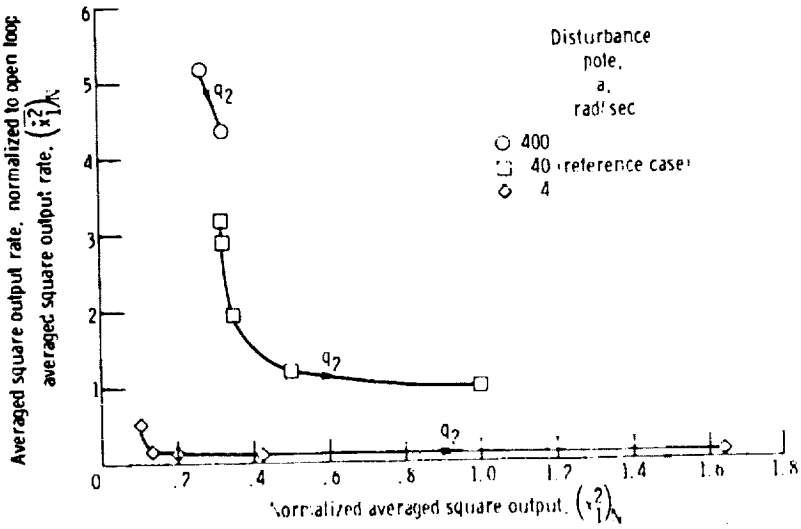

Figure 7. - Comparison of normalized averaged square output and output rate for controllers designed for different disturbance pole locations; q_2 designs only. Averaging time T = 1 second; $R_2 = 0$; $R_1 = \rho$ proportional plus integral control

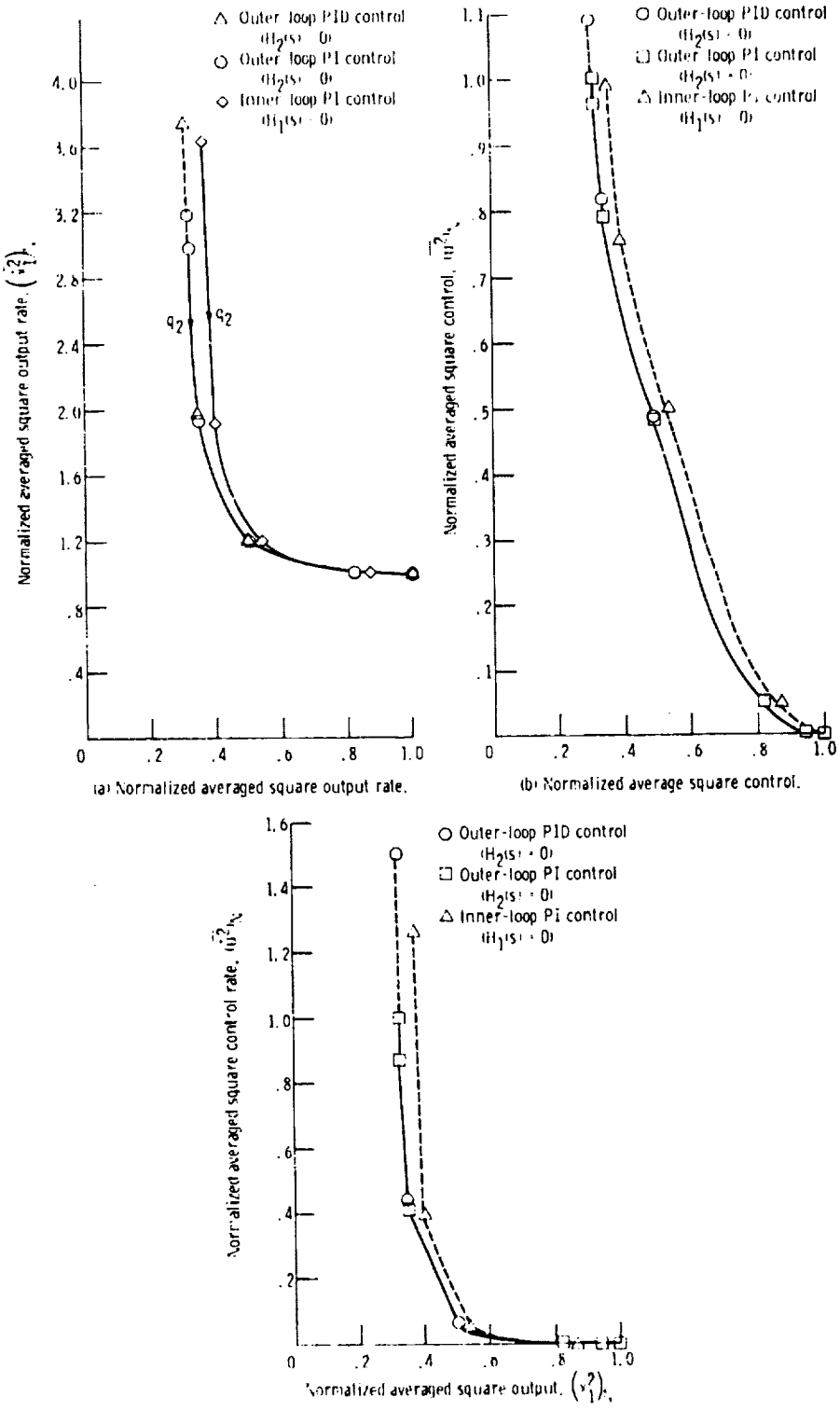

Figure 8. Comparison of normalized averaged square quantities for inner- and outer-loop PI controllers and outer-loop PID controller; q_2 designs only. Averaging time T = 1 second; disturbance rate = 40 radians per second.

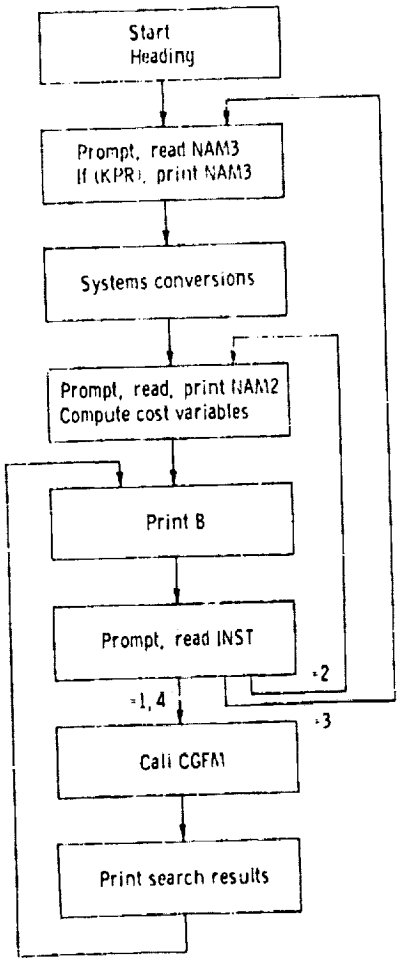

Figure 9. - Flow chart for main program.

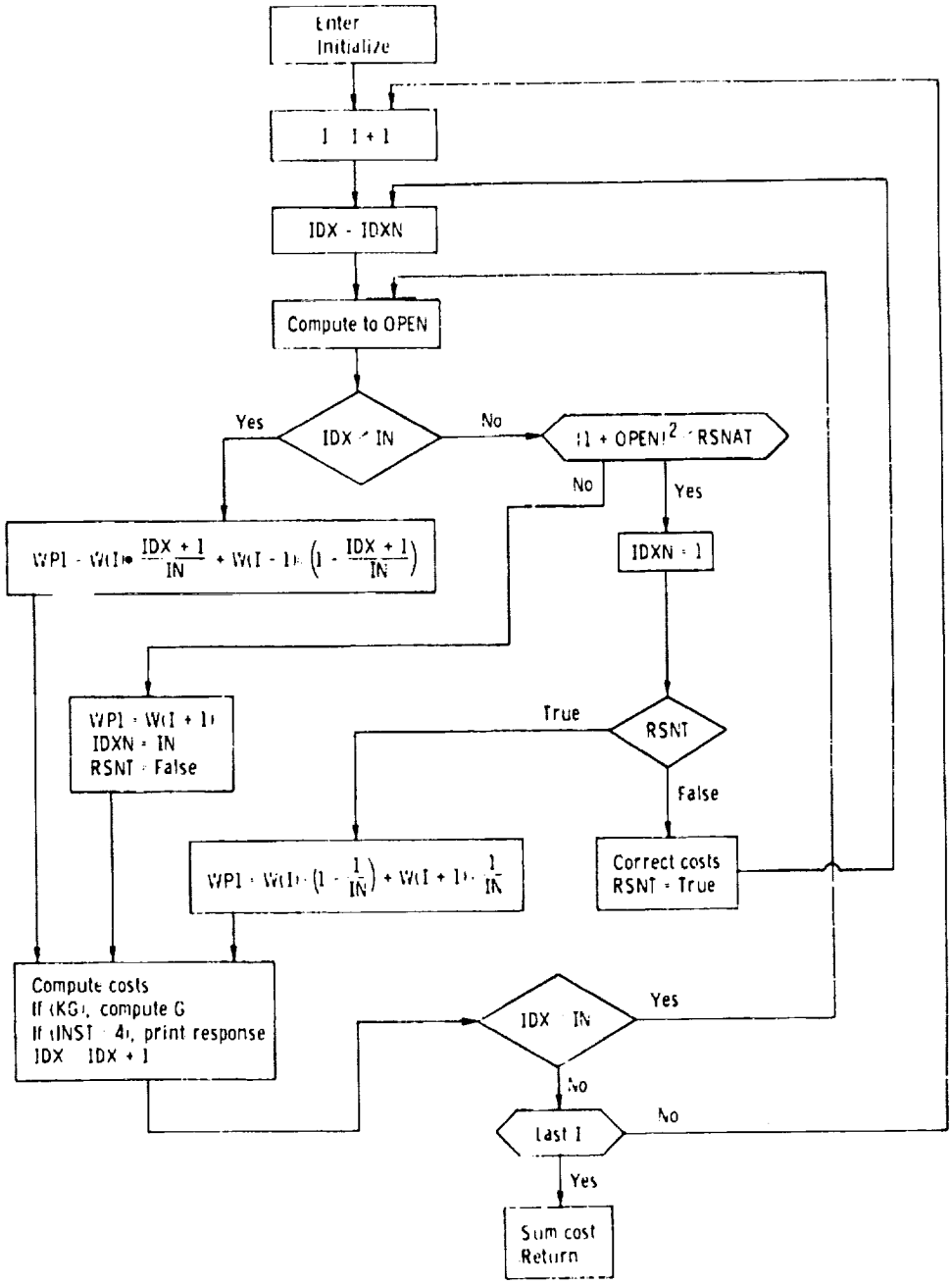

Figure 10. CALFG flow chart.

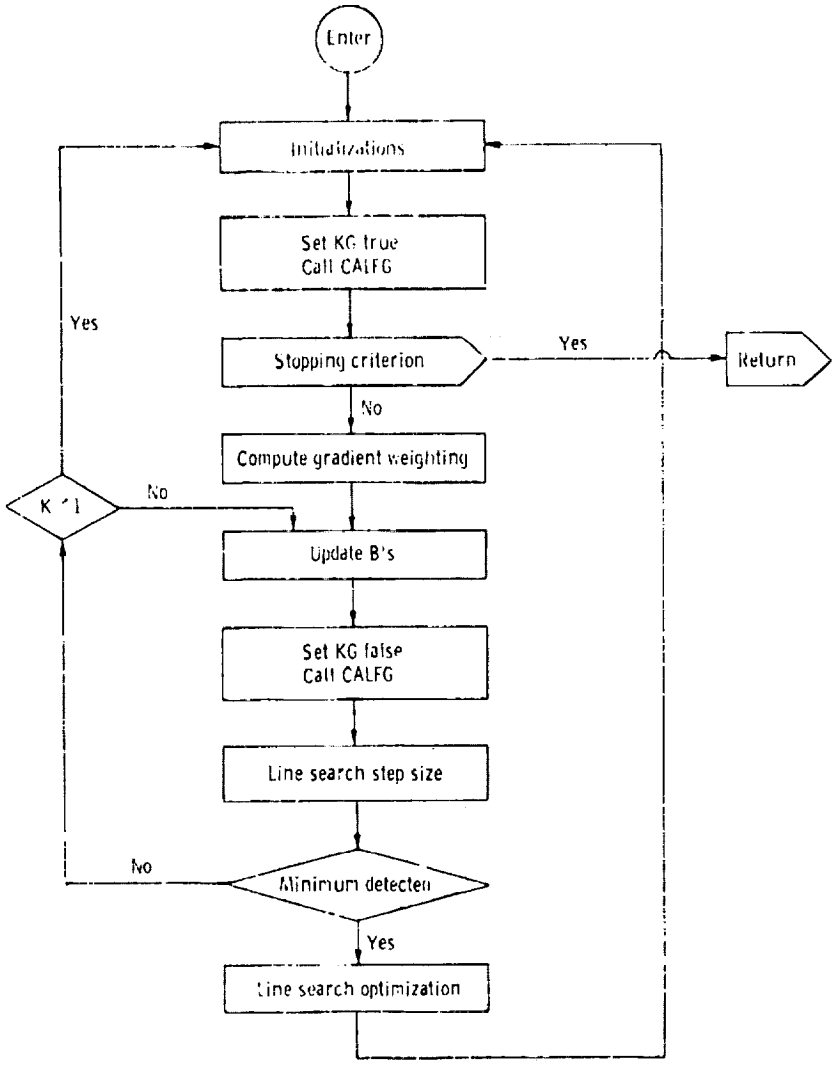

Figure 11. - Flow chart for subroutine CGFM.

E-7210